NAVAL POSTGRADUATE SCHOOL
Monterey, California

THESIS

IMPACT OF HIGH RESOLUTION WIND FIELDS ON COASTAL OCEAN MODELS

by

David Guy Blencoe

September 2001

Thesis Advisor:	Jeff Paduan
Second Reader:	Curt Collins

Approved for public release; distribution is unlimited

Report Documentation Page

Report Date	Report Type	Dates Covered (from... to)
30 Sep 2001	N/A	-

Title and Subtitle Impact of High Resolution Wind Fields on Coastal Ocean Models	**Contract Number**
	Grant Number
	Program Element Number
Author(s) David Guy Blencoe	**Project Number**
	Task Number
	Work Unit Number
Performing Organization Name(s) and Address(es) Research Office Naval Postgraduate School Monterey Ca. 93943-5138	**Performing Organization Report Number**
Sponsoring/Monitoring Agency Name(s) and Address(es)	**Sponsor/Monitor's Acronym(s)**
	Sponsor/Monitor's Report Number(s)
Distribution/Availability Statement Approved for public release, distribution unlimited	
Supplementary Notes	
Abstract	
Subject Terms	
Report Classification unclassified	**Classification of this page** unclassified
Classification of Abstract unclassified	**Limitation of Abstract** UU
Number of Pages 85	

REPORT DOCUMENTATION PAGE			Form Approved OMB No. 0704-0188
Public reporting burden for this collection of information is estimated to average 1 hour per response, including the time for reviewing instruction, searching existing data sources, gathering and maintaining the data needed, and completing and reviewing the collection of information. Send comments regarding this burden estimate or any other aspect of this collection of information, including suggestions for reducing this burden, to Washington headquarters Services, Directorate for Information Operations and Reports, 1215 Jefferson Davis Highway, Suite 1204, Arlington, VA 22202-4302, and to the Office of Management and Budget, Paperwork Reduction Project (0704-0188) Washington DC 20503.			
1. AGENCY USE ONLY ***(Leave blank)***	**2. REPORT DATE** September 2001	**3. REPORT TYPE AND DATES COVERED** Master's Thesis	
4. TITLE AND SUBTITLE: Title (Mix case letters) Impact of High Resolution Wind Fields on Coastal Ocean Models			**5. FUNDING NUMBERS**
6. AUTHOR(S) David Guy Blencoe			
7. PERFORMING ORGANIZATION NAME(S) AND ADDRESS(ES) Naval Postgraduate School Monterey, CA 93943-5000			**8. PERFORMING ORGANIZATION REPORT NUMBER**
9. SPONSORING / MONITORING AGENCY NAME(S) AND ADDRESS(ES) N/A			**10. SPONSORING / MONITORING AGENCY REPORT NUMBER**
11. SUPPLEMENTARY NOTES The views expressed in this thesis are those of the author and do not reflect the official policy or position of the Department of Defense or the U.S. Government.			
12a. DISTRIBUTION / AVAILABILITY STATEMENT Approved for public release; distribution is unlimited.			**12b. DISTRIBUTION CODE**

13. ABSTRACT ***(maximum 200 words)***

The development of a coastal ocean circulation model involves many challenges, including the interaction of complex coastline and topography and the prediction of mesoscale oceanographic features. The Innovative Coastal-Ocean Observing Network (ICON) developed a Monterey Bay ocean circulation model to resolve these challenges. This study examines two different ICON model cases. The first ICON model case was forced with the 100 km NOGAPS winds while the other was forced with the 9 km COAMPS winds. The comparison demonstrated that the 9 km COAMPS-forced case produced better resolution of the ocean mesoscale. This was shown through examination of the daily sea surface temperature fields and the daily surface ocean currents. Time series of sea surface temperature showed a strong seasonal cycle. After removal of the seasonal cycle, the existence of mesoscale features was even more dramatic. A case study at Pt. Sur showed the evolution of mesoscale features associated with an upwelling event.

14. SUBJECT TERMS COAMPS, NOGAPS, POM, Coastal Ocean Modeling			**15. NUMBER OF PAGES** 71
			16. PRICE CODE
17. SECURITY CLASSIFICATION OF REPORT Unclassified	**18. SECURITY CLASSIFICATION OF THIS PAGE** Unclassified	**19. SECURITY CLASSIFICATION OF ABSTRACT** Unclassified	**20. LIMITATION OF ABSTRACT** UL

NSN 7540-01-280-5500

Standard Form 298 (Rev. 2-89)
Prescribed by ANSI Std. 239-18

THIS PAGE INTENTIONALLY LEFT BLANK

Approved for public release; distribution is unlimited

IMPACT OF HIGH RESOLUTION WIND FIELDS ON COASTAL OCEAN MODELS

David G. Blencoe
Lieutenant, United States Navy
B.S., University of South Carolina, 1994

Submitted in partial fulfillment of the
requirements for the degree of

MASTER OF SCIENCE IN METEOROLOGY AND OCEANOGRAPHY

from the

NAVAL POSTGRADUATE SCHOOL
September 2001

Author: _____
David G. Blencoe

Approved by: _____
Jeff Paduan, Thesis Advisor

_____
Curt Collins, Second Reader

_____
Mary Batteen, Chairman
Department of Oceanography

THIS PAGE INTENTIONALLY LEFT BLANK

ABSTRACT

The development of a coastal ocean circulation model involves many challenges, including the interaction of complex coastline and topography and the prediction of mesoscale oceanographic features. The Innovative Coastal-Ocean Observing Network (ICON) developed a Monterey Bay ocean circulation model to resolve these challenges. This study examines two different ICON model cases. The first ICON model case was forced with the 100 km NOGAPS winds while the other was forced with the 9 km COAMPS winds. The comparison demonstrated that the 9 km COAMPS-forced case produced better resolution of the ocean mesoscale. This was shown through examination of the daily sea surface temperature fields and the daily surface ocean currents. Time series of sea surface temperature showed a strong seasonal cycle. After removal of the seasonal cycle, the existence of mesoscale features was even more dramatic. A case study at Pt. Sur showed the evolution of mesoscale features associated with an upwelling event.

THIS PAGE INTENTIONALLY LEFT BLANK

TABLE OF CONTENTS

I. INTRODUCTION 1
- A. CALIFORNIA CURRENT AND MONTEREY BAY CIRCULATION OVERVIEW 2
- B. GLOBAL MODEL AND NESTED MODEL OVERVIEW 3
  - 1. Navy Operational Global Atmospheric Prediction System (NOGAPS) 3
  - 2. Coupled Ocean/Atmosphere Mesoscale Prediction System (COAMPS) 4
- C. MONTEREY BAY COASTAL OCEAN PROGRAM 6
  - 1. Monterey Bay Area (ICON) Ocean Circulation Model 6
- D. FOCUS OF THESIS WORK 7

II. DETAILED BACKGROUND OF TOOLS USED 15
- A. BACGROUND INFORMATION OF THE ICON OCEAN CIRCULATION MODEL 15
- B. NAVY OPERATIONAL GLOBAL ATMOSPHERIC PREDICTION SYSTEM (NOGAPS) 16
- C. COUPLED OCEAN/ATMOSPHERE MESOSCALE PREDICTION SYSTEM (COAMPS) 18

III. RESULTS 21
- A. ICON MODEL RUNS 21
- B. ANNUAL DATA 22
- C. SEASONAL DATA 25
- D. REMOVING THE SEASONAL CYCLE – HIGHPASS DATA 26
- E. UPWELLING CASE STUDY 28

IV. CONCLUSIONS 57

LIST OF REFERENCES 67

INITIAL DISTRIBUTION LIST 71

THIS PAGE INTENTIONALLY LEFT BLANK

LIST OF FIGURES

Figure 1. Overview Of The California Current System……. 8
Figure 2. Coastal Features Of Monterey Bay And Ocean Observing Locations..... 9
Figure 3. COAMPS Triple Nested Grid..……. 10
Figure 4. ICON Model Domain From Shulman (2001)…… . 11
Figure 5. Northern Upwelling Location…….. ...……. 12
Figure 6. Southern Upwelling Location……..……. 13
Figure 7. SST From COAMPS-Forced ICON Model Run For Day 87 (28 March) 1999 Showing Cold Water Upwelling Near The Coast……. 30
Figure 8. SST From COAMPS-Forced ICON Model Run For Day 94 (4 April) 1999 Showing The Presence Of A Cold Water Filament…… 31
Figure 9. Surface Velocity Vectors From COAMPS-Forced ICON Model Run For Day 83 (24 March) 1999 Showing a Mesoscale Eddy Near 36°N, 122°W 32
Figure 10. COAMPS-Forced ICON Model Sea Surface Temperature Average (Annual)……. ..... ……33
Figure 11. NOGAPS-Forced ICON Model Sea Surface Temperature Average (Annual)..……. ..... …….34
Figure 12. COAMPS-Forced ICON Model Sea Surface Temperature Standard Deviation (Annual)……..... ……...35
Figure 13. NOGAPS-Forced ICON Model Sea Surface Temperature Standard Deviation (Annual)….……. ..... ……..36
Figure 14. COAMPS-Forced ICON Model Surface Velocity Vectors Average (Annual)……..……. ... …….37
Figure 15. NOGAPS-Forced ICON Model Surface Velocity Vectors Average (Annual)……..……. ..... …….38
Figure 16. COAMPS-Forced ICON Model U And V Surface Velocity Standard Deviation (Annual)....……...39
Figure 17. NOGAPS-Forced ICON Model U And V Surface Velocity Standard Deviation (Annual)..……....……..39
Figure 18. Observed Surface Winds At Mooring M3 And M2 (Days 194 To 202)……..40
Figure 19. COAMPS-Forced ICON Model Sea Surface Temperature Average (Seasonal)…….…41
Figure 20. NOGAPS-Forced ICON Model Sea Surface Temperature Average (Seasonal)……..42
Figure 21. COAMPS-Forced ICON Model Surface Velocity Vectors Average (Seasonal)…..……43
Figure 22. NOGAPS-Forced ICON Model Surface Velocity Vectors Average (Seasonal)…….……44
Figure 23. Fluctuation Of Sea Surface Temperature At Gridpoint 2806 And 627……..…45
Figure 24. Energy Density Spectrum……..46
Figure 25. High Pass Filtered COAMPS-Forced ICON Model Sea Surface Temperature Standard Deviation (Seasonal)……47

Figure 26. High Pass Filtered NOGAPS-Forced ICON Model Sea Surface Temperature Standard Deviation (Seasonal)……48
Figure 27. SST From COAMPS-Forced ICON Model Run For Day 81 (22 March) 1999 Showing Warm Water Concentration At The Coast……49
Figure 28. SST From COAMPS-Forced ICON Model Run For Day 87 (28 March) 1999 Showing Upwelling Of Cold Water At Pt. Sur……50
Figure 29. SST From COAMPS-Forced ICON Model Run For Days 88-91 (29 March - 2 April) 1999 Showing Filament And Eddy Formation……51
Figure 30. Surface Velocity Vectors From COAMPS-Forced ICON Model Run For Day 81 (22 March) 1999 Showing Concentration Of Warm Water Along Coast……..……....52
Figure 31. Surface Velocity Vectors From COAMPS-Forced ICON Model Run For Day 87 (28 March) 1999 Showing Upwelling of Cold Water At Pt. Sur…….53
Figure 32. Surface Velocity Vectors From COAMPS-Forced ICON Model Run For Days 88-91 (29 March - 2 April) 1999 Showing Filament And Eddy Formation……..54
Figure 33. High Pass Filtered COAMPS-Forced ICON Model Run For Day 84 (25 March) 1999 Showing Concentration Of Warm Water At Pt. Sur…….55
Figure 34. High Pass Filtered COAMPS-Forced ICOM Model Run For Days 92-95 (3 April - 6 April) 1999 Showing The Progression Of Upwelled Water …….56
Figure 35. 9km COAMPS Winds From COAMPS Run For Day 132 (12 May) 1999…..61
Figure 36. SST For COAMPS-Forced ICON Model Run For Day 132 (12 May) 1999 Showing Upwelled Cold Water At Pt. Sur……..…….62
Figure 37. Surface Velocity Vectors For COAMPS-Forced ICON Model Run For Day 132 (12 May) 1999 Showing Upwelled Cold Water At Pt. Sur……63
Figure 38. Aircraft Derived Winds, SST, And Air Temperature Near Pt. Santa Cruz…..64
Figure 39. Computed Wind Stress Curl Near Pt. Santa Cruz……65

LIST OF TABLES

Table 1. ICON Model Runs Without Surface Current Assimilation. 21

THIS PAGE INTENTIONALLY LEFT BLANK

ACKNOWLEDGMENTS

I would like to thank several people for their assistance and their support throughout the entire process of my thesis project. First and foremost I would like to thank my wife Katti and children Christopher and Joshua for their patience and understanding on those days when I seemed so frustrated by the apparent lack of progress, and through all the late hours at the end. I love you. I would like to thank my thesis advisor, Jeff Paduan, for his direction, taking the time to ensure that I understood what he was saying, and for the late hours spent finishing up. Lastly, I would like to thank Mike Cook, the MATLAB Master. If it weren't for his extensive expertise in MATLAB and his tolerance for repeated questions, I never would've finished this project.

I. INTRODUCTION

The United States Navy continues to operate more and more in a littoral environment, which continues to challenge the effectiveness of their operations. In order to complete their mission the accuracy of environmental data and prediction is a primary concern. One of the tools being used is an ocean circulation model, which is constantly being modified and refined for use in coastal ocean regions. There are many challenges and difficulties involved in creating an ocean circulation model for these littoral regions. Numerous considerations must be taken into account that would not necessarily be relevant in an ocean circulation model for the open ocean. For example, some of the considerations that must be accounted for are: variations in the coastline, coastal topography, the existence of coastal currents, the advection of eddies through the model domain, cold and warm water filaments extending from the shore, upwelling locations and events, and upwelling-induced eddy formation. Figure 1 shows an image of the California Current System that illustrates these features.

Variations in the coastline can be defined as coastal headlands, for example Point Sur, or bays, in this case of this paper, Monterey Bay (Figure 2). The existence of headlands combined with specific wind directions can cause cold or warm water filaments that transfer water away from the coast, and are areas favorable to upwelling which can induce eddies that propagate throughout the domain. These eddies are specific to upwelling areas and will be discussed later in the paper. The existence of bays of the size of Monterey Bay can influence water properties (eg. sea surface temperature), can influence coastal winds, and can create their own circulation. The existence of a coastal current, such as the California Current or the California Undercurrent, can produce additional features that will influence model output. The north-to-south flow of the California Current and California Undercurrent are not constant and meanders and eddies will propagate throughout the model domain as well. The characteristics of these eddies are different from those of upwelling-induced eddies touched on earlier.

Another consideration, separate from the physical properties just mentioned, is the resolution of the model and forcing parameters. The difference in resolution between forcing parameters on the model from the Navy Operational Global Atmospheric Prediction System (NOGAPS) and the Coupled Ocean/Atmosphere Mesoscale Prediction System (COAMPS) can lead to the development of different features seen in the model output. A comparison between the ocean circulation model output using NOGAPS as a forcing mechanism and the model output using COAMPS as a forcing mechanism is the primary focus of this paper.

A. CALIFORNIA CURRENT AND MONTEREY BAY CIRCULATION OVERVIEW

A complex and varied coastline and regions of irregular, steep topography characterize the California coast. The Monterey Bay region is of particular interest to many different groups. Monterey Bay is characterized by its own micro-scale circulation. Local upwelling events and strong land/sea breeze influence circulation patterns throughout the area. During spring and summer, near-surface water offshore of the Monterey Bay flows mostly southward due to local equatorward wind stress and the influence of the California Current (CC) (see, Rosenfeld et al., 1994). According to Ramp et al. (1997) and Collins et al. (2000), there are two narrow, poleward flowing boundary currents around the Monterey Bay area: the Inshore Countercurrent (IC) (sometimes referred to as the Davidson Current), and the California Undercurrent (CU). The water properties of the CC, IC, and CU currents are determined by four water masses (Lynn and Simpson, 1987): the Pacific Subarctic (in upper 200 m), the North Pacific Central and Coastal Upwelled water masses and in the subsurface by the Equatorial Pacific. Analysis in the surface current data derived from HF radar (CODAR) and CTD observations indicated a presence of large internal tides in the Monterey Canyon. All the above mentioned atmospheric and oceanographic conditions and processes make the Monterey Bay area both interesting and challenging for numerical modeling. A numerical study of barotropic and internal tides has been reported in Petruncio (1998) and Rosenfeld et al. (1999). Ly et al. (1999) modeled the Monterey Bay region response

to wind forcing and tides, and Lewis et al. (1998), modeled the tidal wind driven flow with assimilation of CODAR derived surface currents.

B. GLOBAL MODEL AND NESTED MODEL OVERVIEW

1. Navy Operational Global Atmospheric Prediction System (NOGAPS)

The following quote from Baker et al. (1998) outlines the importance of the capability of the Navy's NOGAPS numerical weather prediction system.

> Accurate weather analysis and prediction have been recognized as indispensable capabilities of modern military forces to attain more efficient use of resources and weapon systems and to realize reduced weather-related damage and fuel costs. Now the Navy with the Navy Operational Global Atmospheric Prediction System has been given the primary responsibility for DOD's global analysis and prediction capability.

NOGAPS has undergone many changes and updates to improve its ability to accurately predict global weather patterns since its inception in August of 1982. As stated earlier, the United States Navy needs accurate global atmospheric prediction. NOGAPS not only provides forecasts that provide guidance for world wide naval operations, but it also provides the forcing and boundary conditions for a large number of atmospheric and oceanographic applications. Some of the oceanographic programs that are dependent on the global atmospheric fields are the Navy's ice prediction models (Hibler 1979; Gerson 1975), the ocean wave spectral models (Clancy et al. 1986), the thermodynamic ocean prediction system (Clancy and Martin 1981; Clancy and Pollak 1983), and the prediction of the ocean currents (Heburn and Rhodes 1987). These programs in turn provide input to other applications that provide the Navy and Coast Guard with ship routing and sea search and rescue information. Among the atmospheric uses of the global atmospheric products are the regional atmospheric model (Hodur 1987), the tropical cyclone track prediction programs (Harrison 1981; Hodur and Burk 1978), and the optimum path aircraft routing system (OPARS) for Navy and Coast Guard flight operations. Spectral models, such as NOGAPS, have proven themselves extremely accurate and efficient in predicting the general circulation of the atmosphere. Currently there are many operational spectral models. Of these, the European Centre for Medium

Range Forecasts (ECMWF) is the recognized leader in global atmospheric prediction. The lessons learned by the ECMWF center have been utilized in developing NOGAPS.

Initially NOGAPS was a nine-layer, finite difference model with a horizontal resolution of 2.4° X 3.0°. The major components of the model's dynamics and physics were based on those originally developed for the UCLA General Circulation Model (Arakawa and Lamb 1977). The operational forecasts were run to five days with the model showing skill to 96 hours. A major correction, NOGAPS 2.2, was implemented in July 1986 to correct some apparent deficiencies in the ground temperature and wetness parameterizations. In January 1988 a global spectral model, NOGAPS 3.0, replaced the finite-difference version, 2.2. In March 1989, several major corrections to the parameterizations were implemented, for the 3.1 version of the model. The horizontal and vertical resolutions of 3.0 and 3.1 were the same. In August 1989, the horizontal resolution of the model was increased to 79 wave triangular truncation (T79), corresponding to a 1.5° transform grid. This version of NOGAPS is designated as 3.2. The model parameterizations are the same as 3.1. The other important change in 3.2 was the introduction of a spectral filter in the presence of high winds to allow longer model time steps. On 24 June 1998, NOGAPS was upgraded to version 4.0. The primary change was an increase in the number of vertical levels from 18 to 24.

The resolution of NOGAPS used for forcing the ICON model output in this study was 100 km grid resolution.

2. Coupled Ocean/Atmosphere Mesoscale Prediction System (COAMPS)

Improved understanding of physical processes, dramatic improvements in computer technology, increased observational networks, and the availability of detailed surface parameters have made possible the numerical prediction of some meso-β-scale atmospheric phenomena. Predictions on these scales imply that the hydrostatic approximation may be invalid at times, particularly for convection and smaller-scale topographic features where the vertical wavelength is a significant fraction of the horizontal wavelength and therefore the vertical acceleration term cannot be ignored. Use of nonhydrostatic models is necessary for the prediction of atmospheric scales of

motion at and below meso-β, which is typically at and below 9km in the atmosphere near topography. These phenomena can be created in two ways, either through external or internal forcing. The externally forced modes can result from the interaction of the flow with sharp terrain, irregularly shaped coastlines, and/or sharp gradients in parameters such as the surface roughness, surface albedo, ground temperature, soil moisture, and sea surface temperature. The irregularity of the California coastline and its topography is a direct example of the externally forced modes. Internally forced modes can result from instabilities characteristic of some flows or through scale interactions within the flow. The prediction of the externally forced modes depends critically on the correct specification of the lower boundary. Over water, this implies the use of a detailed description of the sea surface temperature, and in cases where there exist strong interactions between the atmosphere and ocean, an ocean model should be coupled to the atmospheric model to incorporate changes to the ocean temperature and currents as they occur.

The Naval Research Laboratory (NRL) has developed a system that is capable of predicting mesoscale atmospheric phenomena down to the meso-β scale that are externally forced through interactions with the lower boundary. This system is referred to as COAMPS and includes an atmospheric data assimilation system comprised of data quality control, analysis, initialization, and nonhydrostatic atmospheric model components, as well as a hydrostatic ocean model. COAMPS is a three-dimensional system and the two models can be used separately or in a fully coupled mode.

There are several significant differences between COAMPS and NOGAPS. The most significant difference is that, while NOGAPS is a global spectral model with a 100 km resolution, COAMPS is a regional model that is triple nested with three different grid resolutions working in tandem. The term triple nested refers to the setup and structure of the model and the relationship between the three grids. COAMPS begins with an initial grid with an 81 km resolution, then a second grid with a 27 km resolution, and a final grid with a 9 km resolution (Figure 3). The resolution of COAMPS used in forcing the ICON model output is a 9 km grid resolution.

C. MONTEREY BAY COASTAL OCEAN PROGRAM

The partnership that the original ICON modeling effort was completed under is called the Innovative Coastal-Ocean Observing Network (ICON), which is a component of the National Ocean Partnership Program (NOPP). The ICON network is composed of several institutions, to include: the Naval Postgraduate School (NPS), the Monterey Bay Aquarium Research Institute (MBARI), California State University at Monterey Bay (CSUMB), the University of Southern Mississippi (USM), the University of Michigan (UM), HOBI Labs, CODAR Ocean Sensors Ltd. (COS), and the Naval Research Laboratory (NRL). Some of the components of the ICON network include: sea surface temperatures, ocean color/productivity, surface currents, subsurface currents, ocean acoustic observatory, meteorology, and ocean forecasting. The goals of the cooperative efforts of the partnership are to make observations of critical ocean parameters, retrieve data in near-real time, assimilate the data into predictive models and to forecast ocean conditions. These goals are in support of sanctuary management, fisheries management, littoral warfare/national security, and wave and weather forecasting. The main objective of the ICON model development is demonstration of the capability of a high resolution model to track the major mesoscale ocean features in the Monterey Bay area when constrained by the measurements and nested within a regional larger scale model.

1. Monterey Bay Area (ICON) Ocean Circulation Model

The phases of the ICON modeling program were: 1.) The development of a fine-resolution, hydrodynamic model of the Monterey Bay area capable of resolving the temporal and spatial scales of corresponding oceanic processes and bringing together the unique oceanographic data sources available in this area; 2.) The development of technology for coupling the Monterey Bay area model with a larger regional model (Shulman et al. 1999, 2001). The regional model that the ICON model is coupled to is the Pacific West Coast (PWC) model which is driven by the Navy's Global Layered Ocean model.

This study discussed results from model simulations from 1995 and reproduced many of the hydrographic conditions observed in the Monterey Bay area. Included were cool plumes of upwelled water extending from north to south and seaward of Monterey

Bay during May – June 1995, a meandering, alongshore ocean front between the upwelled water and the warmer water of the California current, and at 200 m the northward flow over the continental slope off the Monterey Bay associated with the California Undercurrent. Also the model did well in reproducing the mean water temperatures at a given depth. The model reproduced a strong upwelling and the correct position for cold-water formation near Pt. Sur, CA. The second round of study is focusing primarily on the continued development of the ICON model with assimilation of surface currents from high frequency radars.

D. FOCUS OF THESIS WORK

The primary focus of the thesis was the output from the ICON model for 1999. The output was contained in two different files. Each file included daily sea surface temperatures and surface velocity vectors for all the grid points. One file was produced with forcing by the NOGAPS 100 km resolution wind fields and the second was produced through forcing by the COAMPS 9 km resolution wind fields. Different approaches were used to examine the model output. ICON model output parameters studied within this paper are sea surface velocities and temperature. A comparison was done between the effects of the high resolution (COAMPS) wind forcing and the low resolution (NOGAPS) wind forcing throughout the model domain, shown in Figure 4. The next step was narrowing the focus of the study to regions that displayed a strong upwelling signature along the California coastline. Two upwelling locations were chosen. The first is to the north of the Monterey Bay, near Point Arenas (between 37.3°N and 36.95°N), called the Northern Upwelling Location (Figure 5). The second was to the south of Monterey Bay, near Point Sur (between 36.55°N and 36.2°N), called the Southern Upwelling Location (Figure 6). Comparisons were made between the two locations as to the range of coastline covered, the magnitude of the upwelling events, and the duration. Also noted were the differences in onset indicators, the upwelling signature, and the relaxation of specific upwelling events throughout the year. A specific case study of upwelling from the Southern Upwelling location was then selected for further comparison between NOGAPS and COAMPS and the noticeable effects of the wind resolution difference in forcing of the model.

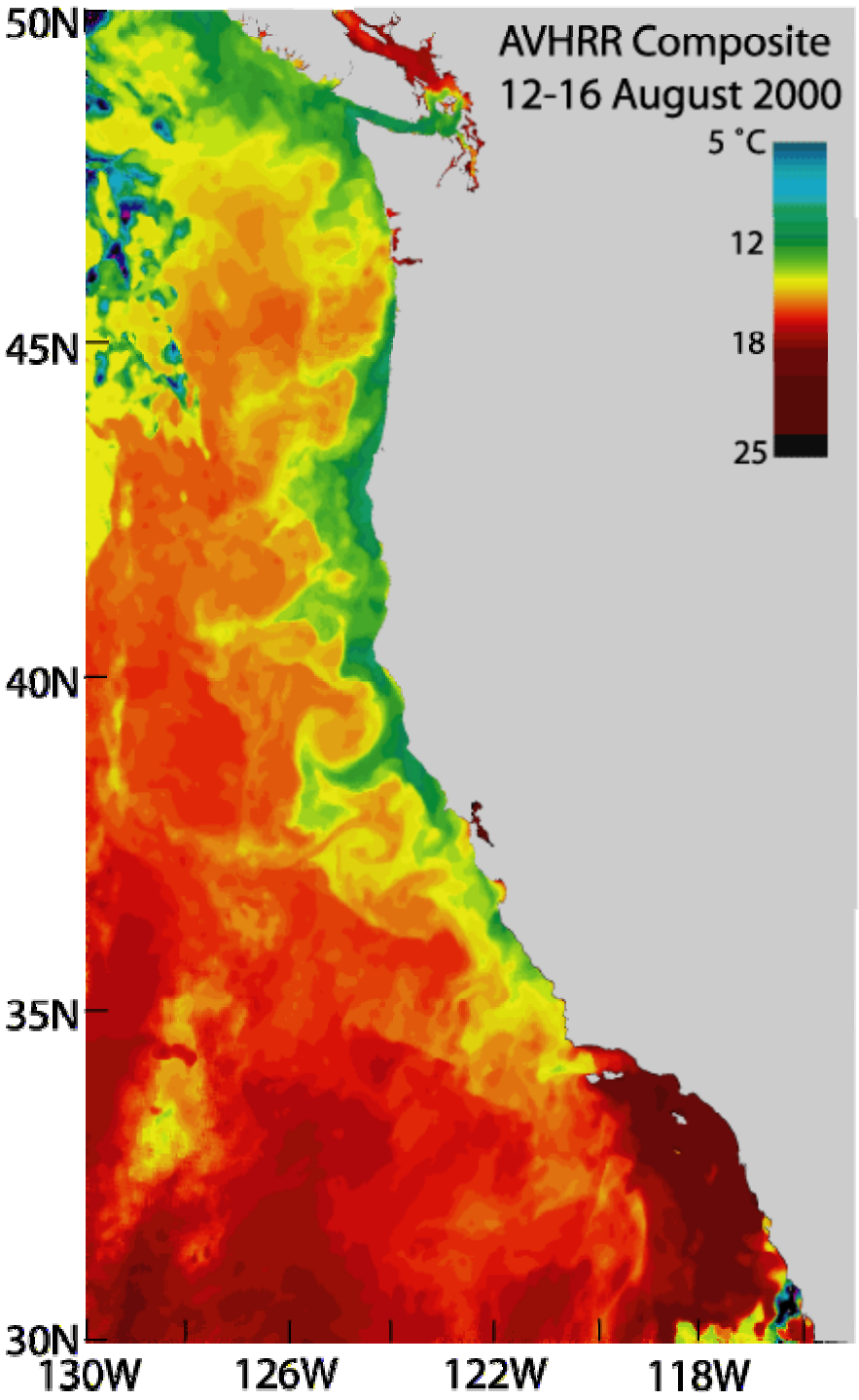

Figure 1. Overview of the California Current System

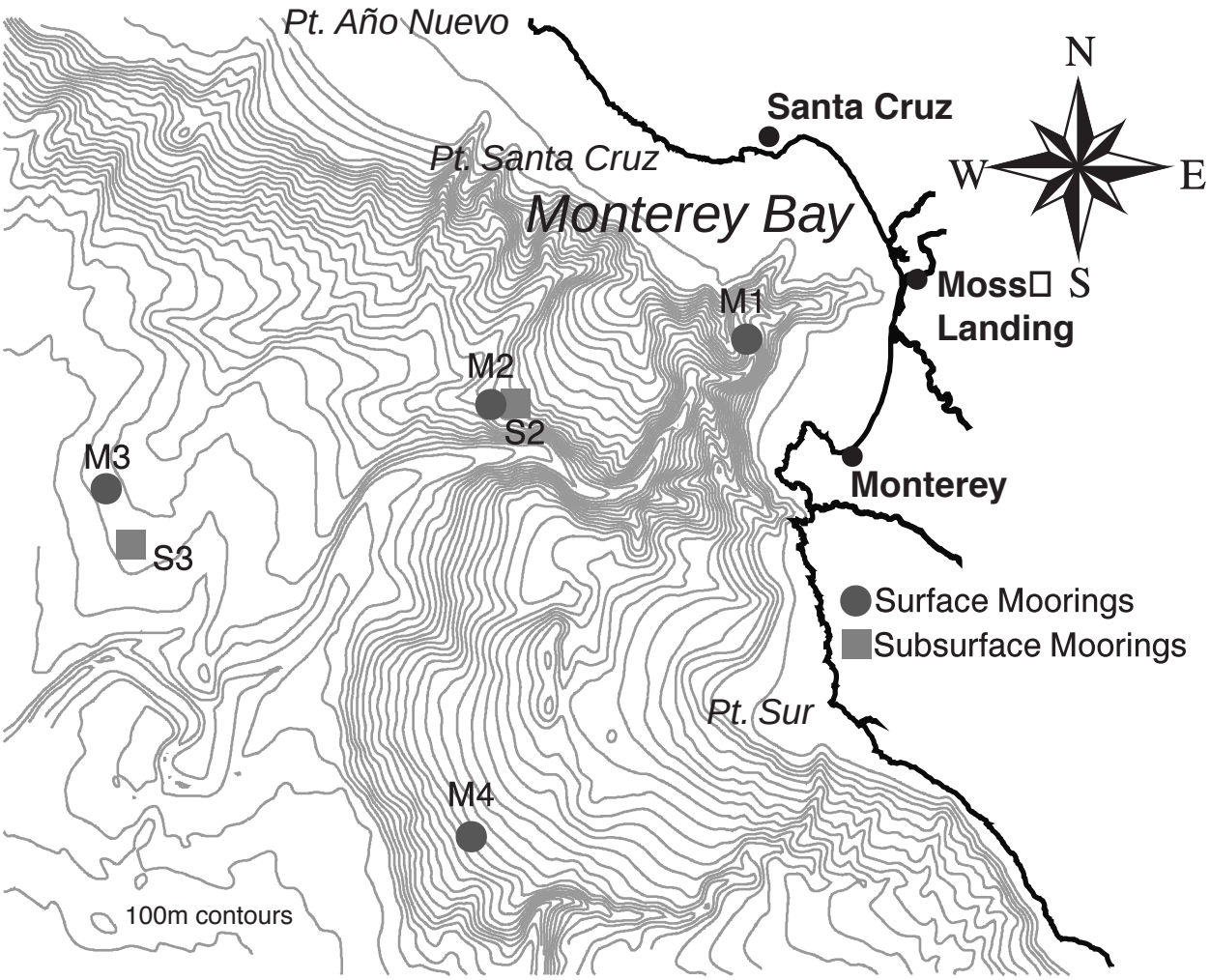

Figure 2. Coastal features of Monterey Bay and ocean observing locations.

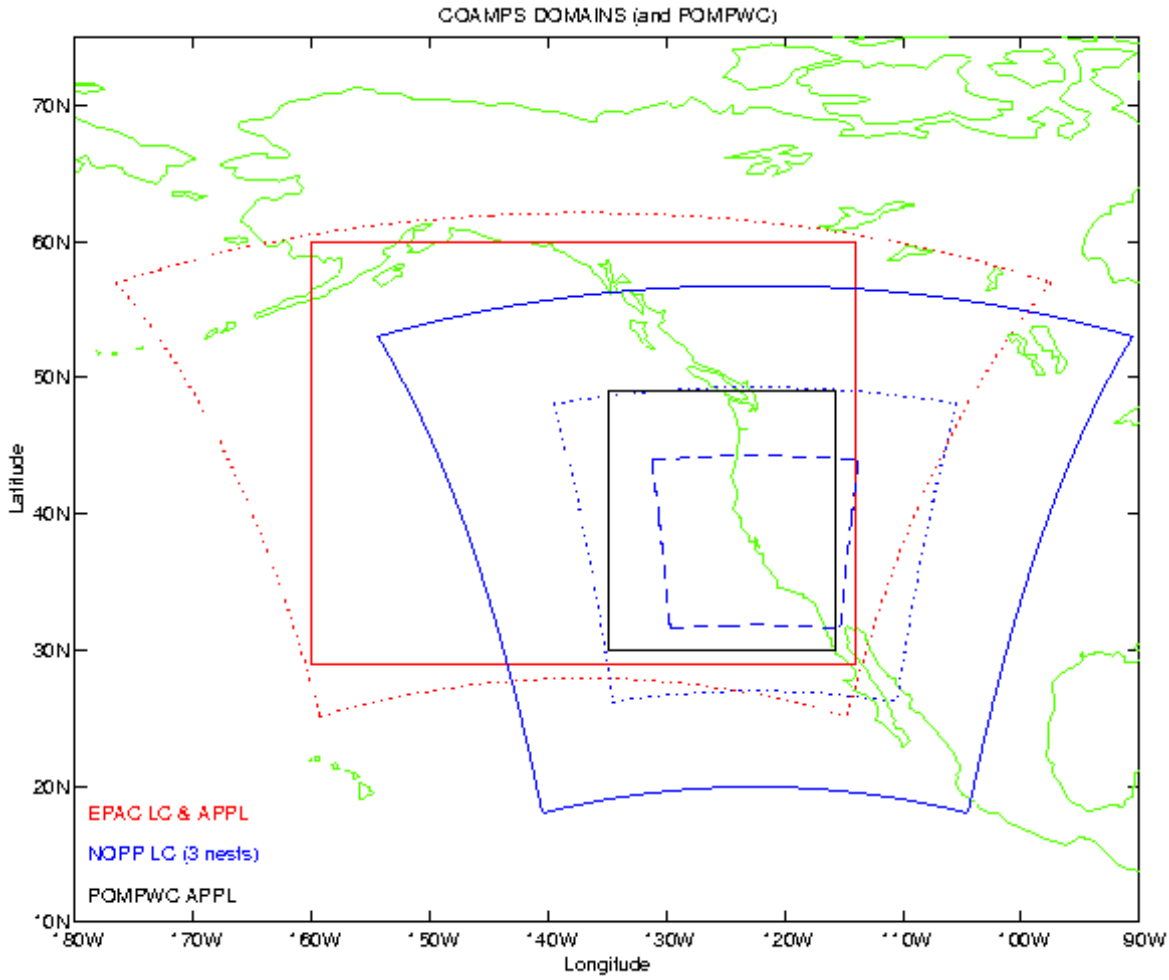

Figure 3. COAMPS triple nested grid (Courtesy of J. Kindle, NRL).

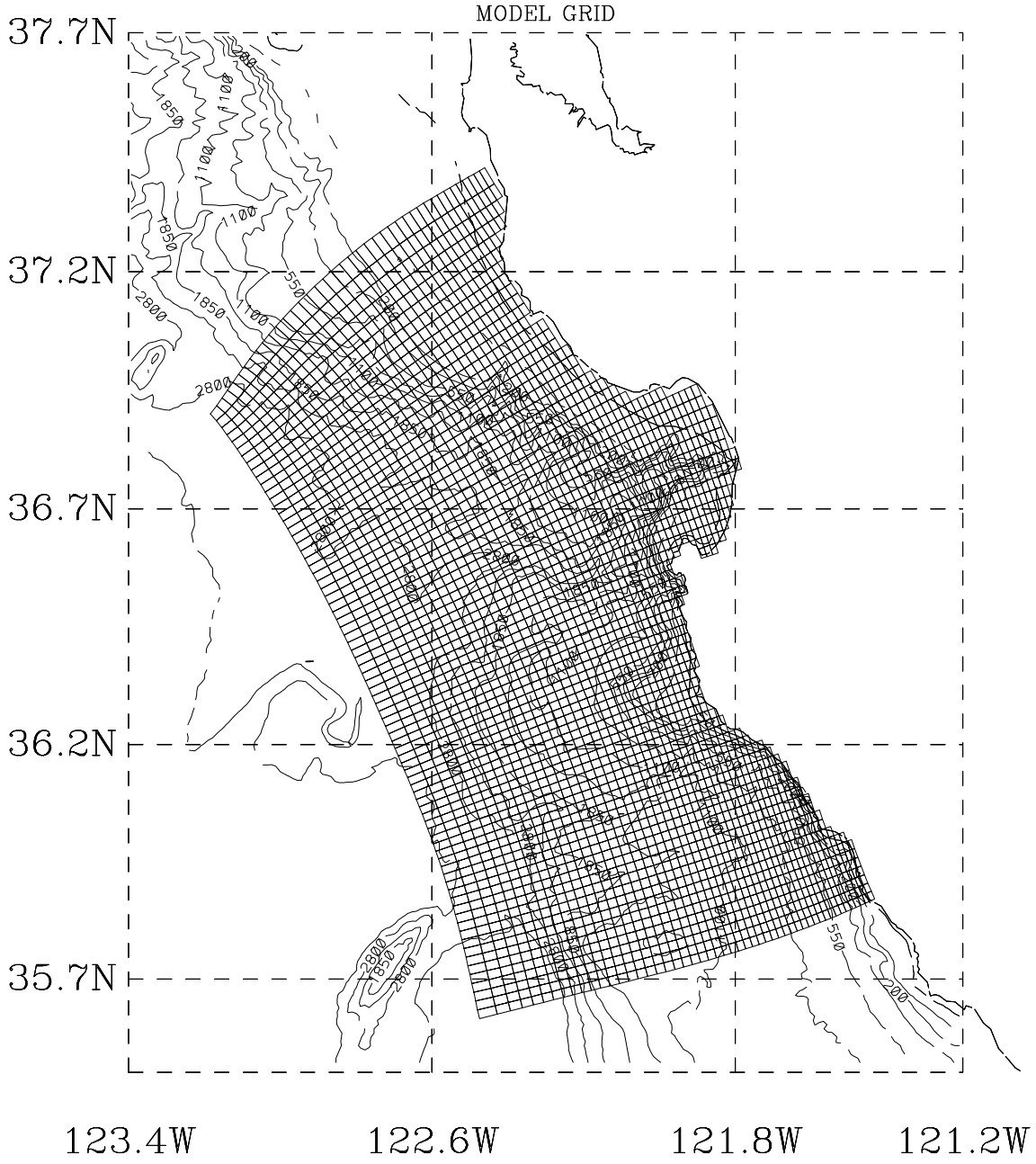

Figure 4. ICON model domain from Shulman et al. (2001).

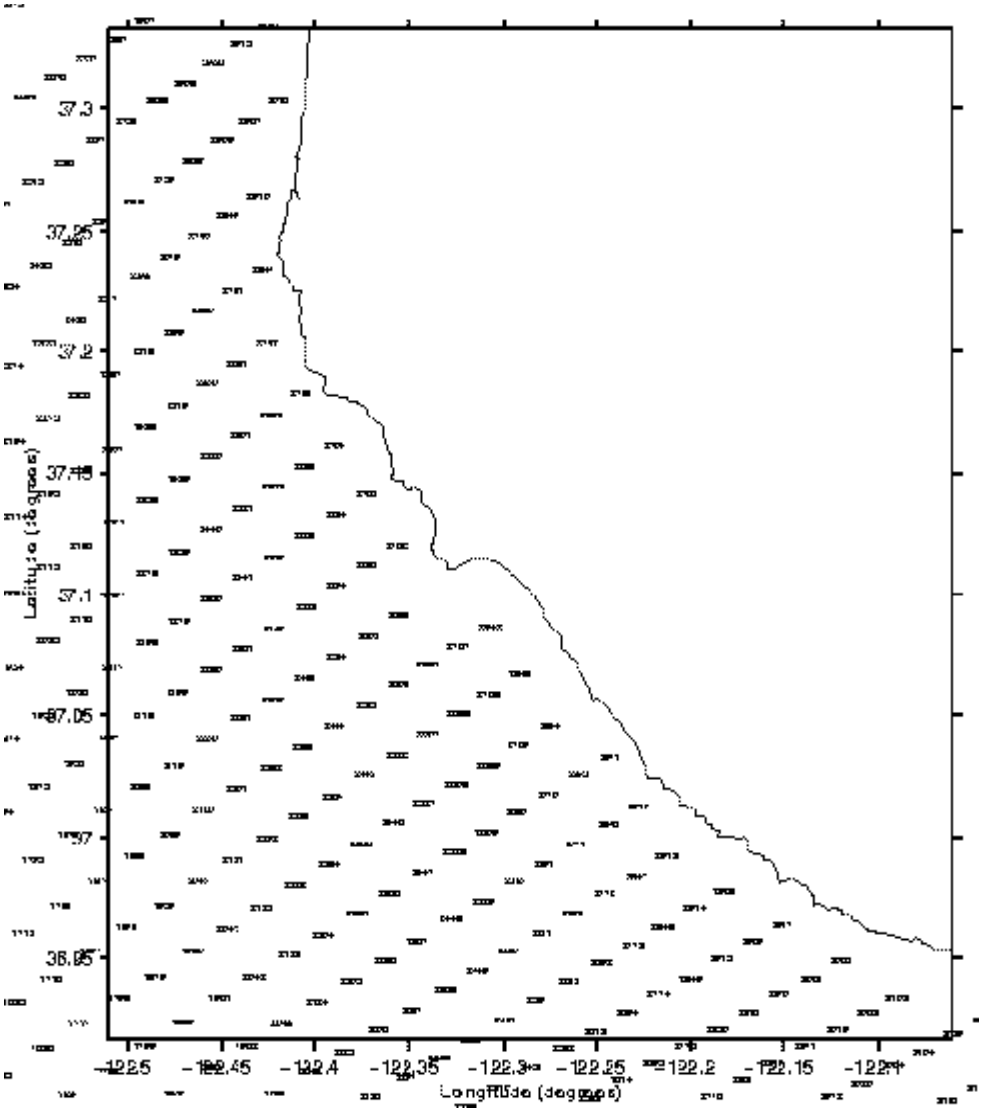

Figure 5 . Northern upwelling location

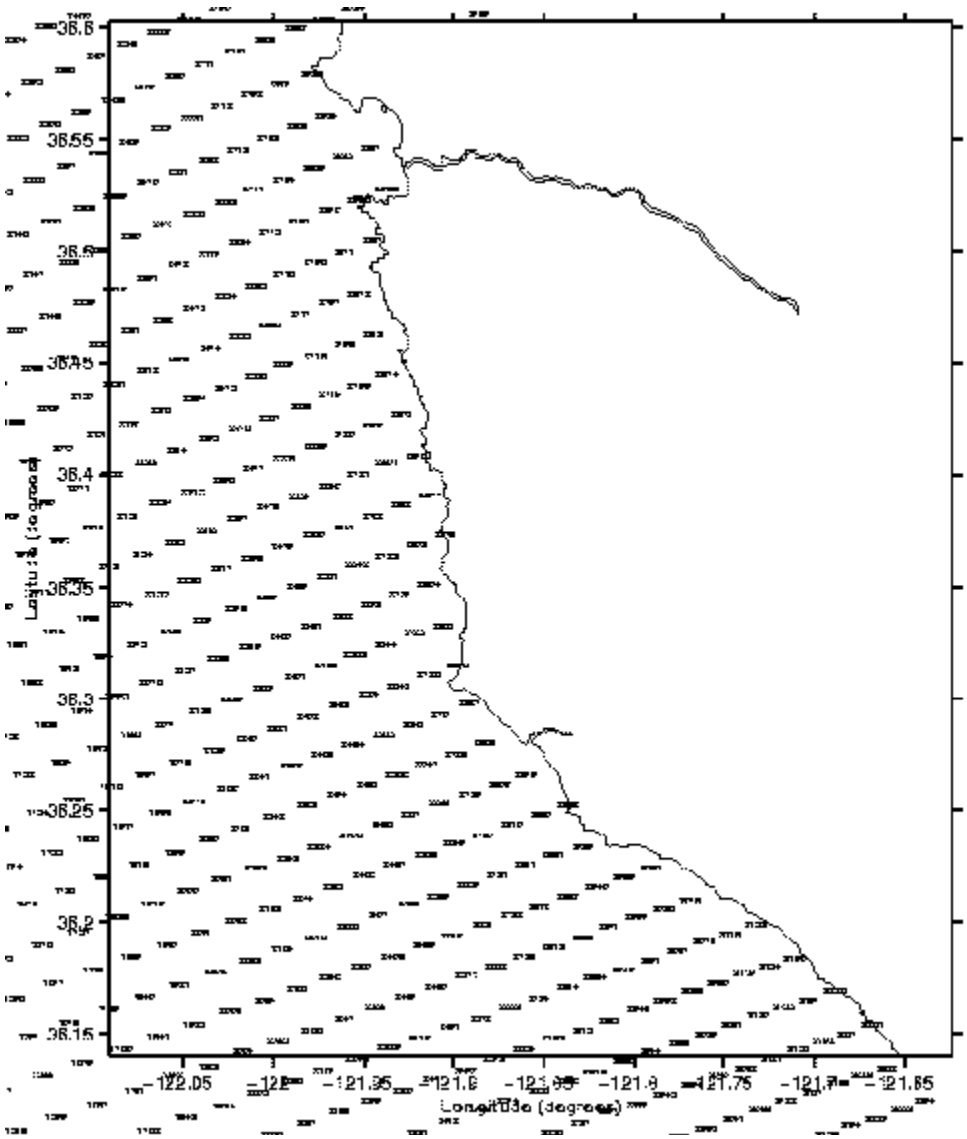

Figure 6. Southern upwelling location

THIS PAGE INTENTIONALLY LEFT BLANK

II. DETAILED BACKGROUND OF TOOLS USED

A. BACKGROUND INFORMATION OF THE ICON OCEAN CIRCULATION MODEL

The orthogonal, curvilinear grid and model bathymetry were presented in Figure 4. The grid had a variable resolution in the horizontal, ranging from 1 – 4 km, with finer resolution around the Bay. The model had thirty vertical sigma levels. Cross-shelf open boundaries of the model (northern and southern) were approximately orthogonal to the isobaths of bathymetry in order for the flow to be almost perpendicular to the cross-shelf open boundaries. A three-dimensional, sigma-coordinate version of the Blumberg and Mellor hydrodynamic model (1987) was used. This is also known as the Princeton Ocean Model (POM). This three-dimensional, free surface model is based on the primitive equations for momentum, salt, and heat. It uses the turbulence closure sub-model developed by Mellor and Yamada, and the Smagorinsky formulation is used for horizontal mixing. Additional information on the model can be found in Blumberg and Mellor (1987).

On the open boundaries, the ICON model was one-way coupled to a larger scale model of PWC defined above (Clancy et al., 1996; Ko et al., 1996, Righi et al., 1999). The PWC model was also based on the POM (explicit, sigma coordinate version) and has a horizontal resolution of 1/12° (around 10 km) and 30 vertical sigma levels. The PWC model domain extended seaward to 135°W longitude, and from 30°N to 49°N in latitude. The model included seven major rivers and was forced with a 12-hourly FNMOC NOGAPS/HR hybrid wind (Clancy et al., 1996). There was a relaxation of the model sea surface temperature (SST) to the observed Multi-Channel SST data (MCSST). An important feature of the PWC model was coupling to a ¼°, global Navy Layered Ocean Model (NLOM) which had an assimilating capability for altimeter sea surface height observations.

The one way coupling between the ICON and PWC models is described in Shulman et al. (2001) as follows:

The barotropic, vertically-averaged velocities on the open boundaries of the Monterey Bay area model were estimated by using the Flather formulation (1976):

$$\bar{u}_n = \overline{u^\circ}_n + (g / H)^{1/2} (\eta - \eta^0) \qquad (1)$$

where u_n is the outward normal component of the velocity on the open boundary at time t (vertically averaged values will be denoted by overbars); $\overline{u^\circ}_n$ is the outward normal component of the velocity on the open boundary at time t estimated from the PWC model results; η is the model sea surface elevation calculated from the continuity equation and located half of a grid inside of the open boundary; η^0 is the PWC model sea surface elevation on the open boundary of the ICON model; H is the water depth on the open boundary, and g is gravitational acceleration. At the same time, an adjustment procedure was used to balance the net transport from the PWC model with the associated variation of sea surface elevation. The available outputs from the PWC model have daily records of sea surface elevation and transports; they were spatially interpolated to the ICON grid by using bivariate interpolation and were linearly interpolated to the ICON model time step in order to form η^0 and $\overline{u^\circ}_n$ in the formulation (1). For temperature on the open boundaries, the advectional boundary conditions were used; advected values were calculated from the PWC profiles of temperature, and interpolated to the ICON model grid. Baroclinic velocities for the ICON model have been determined from a radiation condition for the normal component and advectional boundary condition for the tangential component of the velocity. The ICON model was initialized in June 1994 with a horizontally-constant vertical profile of temperature based on summer conditions in the Bay. The model was forced with FNMOC NOGAPS 12-hourly surface wind stresses and coupled (as described above) at the open boundaries to the Pacific West Coast model. The model was run for 1994-1999 period.

The results of the model simulation are discussed by Shulman et al. (2001). Overall, the model demonstrated a good comparison with observations, particularly with regard to the seasonal cycle.

B. NAVY OPERATIONAL GLOBAL ATMOSPHERIC PREDICTION SYSTEM (NOGAPS)

Baker et al. (1998) gives a detailed background of the NOGAPS model as follows:

The NOGAPS Multivariate Optimum Interpolation (MVOI) analysis is a multivariate statistical analysis scheme patterned after the

volume method developed by Lorenc (1981) for the ECMWF. The analysis is performed on the Gaussian grid of the T159L24 global spectral model on the 16 standard pressure levels from 1000 to 10 mb, inclusive. The maximum number of observations utilized per volume is 600. Besides utilizing conventional observations (surface, rawinsonde, pibal, and aircraft), the analysis makes heavy use of various forms of satellite-derived observations. The analysis utilizes derived soundings from the NOAA and DMSP polar-orbiting satellites as well as DMSP SSM/I total column precipitable water and surface wind speeds. Besides the wind observations derived from the various operational processing centers for the geostationary satellites, the NOGAPS also utilizes high-density multispectral wind observations produced by University of Wisconsin-CIMSS (Goerss et al., 1998).

The NOGAPS forecast model is a global spectral model in the horizontal and energy conserving finite difference (hybrid-sigma coordinate) in the vertical. The model top pressure is set at 1 mb, however the first velocity and temperature level is approximately 5 mb. The dynamics formulation uses vorticity and divergence, virtual potential temperature, specific humidity, and terrain pressure as the dynamic variables. The model is central in time with a semi-implicit treatment of gravity wave propagation and Robert time filtering. The T159L24 model time step begins as 540 seconds, but is dynamically reduced if stratospheric jets go beyond a designated threshold. There is also wave number dependent fourth-order diffusion of vorticity, divergence, and virtual potential temperature. The physics package includes: bulk-Richardson number dependent vertical mixing patterned after ECMWF's vertical mixing parameterization (Louis et al., 1982), a time-implicit Louis surface flux parameterization (Louis, 1979), gravity wave drag (Palmer et al., 1986), shallow cumulus mixing of moisture, temperature, and winds (Tiedtke, 1984), relaxed Arakawa-Schubert cumulus parameterization (Moorthi and Suarez, 1992), convective and stratiform cloud parameterization (Slingo, 1987), and solar and longwave radiation (Harshvardhan, 1989).

The operational T159L24 NOGAPS runs on a CRAY C90 and executes several times each 00Z and 12Z watch, including a six-day forecast completing approximately five and one-half hours past the synoptic time. Lower resolution versions of NOGAPS (T79L18 and T63L18) on a Cray J90 provide the backup to the T159L24 operational run in case of primary super-computing platform outage, the 10 day ensemble runs, and the beta-test version. NOGAPS currently outputs close to 25,000 gridded fields per day. Products from NOGAPS are distributed to a worldwide customer base consisting primarily of U.S. Navy and other DOD entities, the U.S. intelligence community, and various other U.S. government agencies. NOGAPS also provides essential and tailored input to many other models, in particular the Navy's advanced Coupled Ocean/Atmosphere Mesoscale Prediction System (COAMPS),

ocean wave model, sea ice model, ocean circulation model, ocean thermodynamics model, tropical cyclone model, aircraft and ship-routing programs and application programs at both FNMOC and the Air Force Weather Agency (AFWA). The quality controlled observations are another important product from NOGAPS, and are used by the mesoscale model, shipboard analysis and forecasting systems, tactical decision aids, and Fleet users external to the central operational site. Along with the GFDL model and the UK Met Office and Japanese global models, NOGAPS is a primary tropical cyclone forecast tool for the tropical cyclone forecasters at the Joint Typhoon Warning Center and the National Hurricane Center.

Model tendencies that are specific to the area studied in this paper are mentioned for a better understanding of the biases present. In the Pacific, developing low average central pressure error is slightly weak and slow to deepen by 72 hours. Pacific mature lows are 3 to 4 hPa too deep and slow to fill by 72 hours. Since the NOGAPS model tendency is to under-forecast developing oceanic lows and over-forecast mature, filling oceanic lows, the associated surface wind speed forecasts also exhibit similar biases in the areas of higher wind speeds. Surface wind forecasts associated with deepening lows are under-forecast and winds are over-forecast for filling lows. During the cool seasons, upper-level troughs digging southeast out of the Gulf of Alaska to the U.S. West Coast are generally over-forecast (too deep) at the extended forecast period, 96 and 120 hours. Surface highs also have some associated error. The forecast central pressure of the offshore Eastern Pacific high cell is also somewhat strong.

C. COUPLED OCEAN/ATMOSPHERE MESOSCALE PREDICTION SYSTEM (COAMPS)

The atmospheric components of COAMPS are used operationally by the U.S. Navy for short-term numerical weather prediction for various regions around the world. "Features include a globally relocatable grid, user-defined grid resolutions and dimensions, nested grids, an option for idealized or real-time simulations, and code which allows for portability between mainframes and workstations (Hodur, R.M., 1996)." The following gives a detailed description of the COAMPS model (www.nrlmry.navy.mil/projects/coamps/data/overview/index.html).

It represents an analysis-nowcast and short-term (up to 48 hours) forecast tool applicable for any given region of the earth. COAMPS includes an atmospheric data assimilation system comprised of data quality control, analysis, initialization, and nonhydrostatic atmospheric model components and a choice of two hydrostatic ocean models. The atmospheric component of COAMPS can be used for real-data simulations, the analysis can use global fields from NOGAPS or the most recent COAMPS forecast as the first-guess. Observations from aircraft, rawinsondes, ships, and satellites are blended with the first-guess fields to generate the current analysis. For the idealized experiments, the initial fields are specified using an analytic function and/or empirical data (such as a single sounding) to study the atmosphere in a more controlled and simplified setting. The nonhydrostatic atmospheric model includes predictive equations for the momentum, the non-dimensional pressure perturbation, the potential temperature, the turbulent kinetic energy, and the mixing ratios of water vapor, clouds, rain, ice, and snow, and contains advanced parameterizations for boundary layer processes, precipitation, and radiation. The atmospheric model uses nested grids to achieve high-resolution for a given area and contains parameterizations for subgrid scale mixing, cumulus parameterization, radiation, and explicit moist physics. Typical mesoscale phenomena that COAMPS has been applied to includes mountain waves, land-sea breezes, terrain-induced circulations, tropical cyclones, mesoscale convective system, coastal rainbands, and frontal systems.

The COAMPS model domain typically covers a limited area on the earth. The model grid size, usually referred to as grid resolution, can range from a few hundred kilometers (synoptic scale) down to approximately one meter when using the large-scale eddy (LES) mode. Horizontal grid resolution, although user defined, is typically set to a 81 x 27 x 9 km, triple nested grid format. The actual dimensions used depend on the scale of the phenomena the user is interested in simulating. The model dimensions can be set so as to produce any rectilinear pattern and can also be rotated to align with any surface feature, such as the terrain or a coastline. COAMPS can be run with any number of nested grids, with the grid resolution in any mesh one-third that of the next coarser mesh.

A complete ocean data assimilation system for COAMPS is being developed and tested by NRL. This ocean system will contain the following components: data quality control, analysis, initialization, and a forecast model. These components will allow COAMPS to be run so that the atmosphere and ocean systems exchange information on wind stresses, heat fluxes, precipitation, and radiation at prescribed intervals in either a loosely or a tightly-coupled mode.

Because COAMPS uses both real and synthetic observations, and global fields from NOGAPS, the model tendencies are similar to those of NOGAPS. On the synoptic

scale level, COAMPS consistently performs as well as other models, such as NOGAPS, NORAPS, and ECMWF in forecasting synoptic scale events. On the mesoscale level, COAMPS frequently outperforms other models in predicting mesoscale meteorological events, particularly close to land in the littoral zone. The strongest feature of the COAMPS 27-km nest is its ability to capture localized winds and small-scale effects.

III. Results

A. ICON MODEL RUNS

Seven different runs of the ICON model were completed (Table 1) for 1999. In running the model there were three components that had different options to choose from. The first component was the wind forcing that was used during the model run. The 100 km NOGAPS wind fields and 9 km COAMPS wind fields were the two different wind fields forcing the ICON model run. The next component, the surface heat forcing, had three different options to choose from. The three options were: no heat forcing at all, MCSST satellite data assimilation, and COAMPS heat flux. COAMPS heat flux is defined as the COAMPS model predicted latent and sensible heat fluxes. The final component that was variable between the seven model runs was the open body forcing. The open body forcing is the resolution of the winds used to force the larger regional Pacific West Coast model that is one way coupled to the ICON model. Initially the 100 km NOGAPS wind fields were used, but in later runs the 27 km COAMPS wind fields replaced the NOGAPS wind fields.

Table 1. ICON Model Runs without Surface Current Assimilation

Run #	Wind Forcing*	Surface Heat Forcing**	Open Boundary Forcing***
1	NOGAPS	None	PWC0
2	NOGAPS	MCSST	PWC0
3	COAMPS	None	PWC0
4	COAMPS	MCSST	PWC0
5	COAMPS	COAMPS	PWC0
6	COAMPS	None	PWC2
7	COAMPS	COAMPS	PWC2

* 9km resolution COAMPS used
** MCSST surface temperatures always assimilated into PWC but only assimilated in ICON model where indicated.
*** PWC0 is forced with NOGAPS wind; PWC2 is forced with 27 km, operational COAMPS winds.

Model runs one and three in which the surface heat forcing and the open body forcing were the same are evaluated below. There was no heat forcing in either model run, and the NOGAPS wind fields were used for the open body forcing of the larger scale

regional model. The component that differed between the two runs was the resolution of winds used to force the ICON model. In run one, the 100 km NOGAPS wind fields were used and in run three, the 9 km COAMPS wind fields were used. Because no surface heat forcing was used, it is important to note that the model depicted somewhat unrealistic sea surface temperatures. A comparison was made between runs one and three to see which of the two wind fields, NOGAPS or COAMPS, provided the best forcing for the model domain. Specifically, the comparison focused on how upwelling was represented in the sea surface temperature fields and the sea surface velocity fields.

B. ANNUAL DATA

Initially, the entire year of the model output was studied in order to identify regions within the model domain that underwent the most dramatic changes. The output files from the ICON model consisted of daily sea surface temperature and sea surface velocity vectors for each of the 3438 grid points throughout the year. These fields were created from both the NOGAPS and COAMPS run. Daily plots were made in Matlab© and animations were created in order to view the daily evolution of each field. From the animations several different mesoscale features within the model domain were identified. The onset, duration and relaxation of upwelling events can be seen as well as cold-water filaments extending away from the coast, and eddies propagating throughout the domain. Presumably due to the higher resolution in the wind fields, the COAMPS runs produced more mesoscale effects than the NOGAPS run. The NOGAPS run however, was able to reproduce the stronger of the upwelling events. Examples of coastal upwelling (Figure 7), a cold water filament (Figure 8), and a mesoscale eddy (Figure 9) can be seen in the model output.

Annual averages of both the COAMPS (Figure 10) and NOGAPS (Figure 11) sea surface temperature fields were computed and compared. The COAMPS run displayed a sharp upwelling signature along the Big Sur coast (south of Pt. Sur) whereas the NOGAPS run displayed cooler temperatures along the Big Sur coast than the surrounding waters, but nothing as distinguishable as in the COAMPS run. There was a much larger region of very warm water in the southern portion of the model domain in the NOGAPS run than in the COAMPS run. The COAMPS run displayed a sharp boundary between

the warmer water in the southern portion of the model domain and the cooler water in the northern portion. This boundary was not as noticeable in the NOGAPS run.

Standard deviation was computed for runs one (NOGAPS run) and three (COAMPS run) of the sea surface temperature and the sea surface velocity fields. Standard deviation is defined as the square root of the variance, which is the fluctuation about the mean value of each field. The sea surface velocity vectors were plotted separately as the east/west (U velocity vectors) and the north/south (V velocity vectors) directions. Regions containing high values of standard deviation were identified. The high values correlate to large fluctuations within the fields plotted and are related to mesoscale features within the model domain.

The COAMPS and NOGAPS annual sea surface temperature standard deviation plots displayed several interesting areas (Figures 12 and 13, respectively). The first was an area along the coast to the north of Monterey Bay, near Pt. Santa Cruz. A second area was south of Monterey Bay along the Big Sur coastline with the highest values near Pt. Sur. A third area began at the mouth of Monterey Bay and extended to the west/southwest away from the coast. The first two locations correspond to upwelling centers while the third area is probably due to an oceanic front, which separates the cooler water mass from the north from the warmer water entering the model domain from the south. The standard deviation plots also showed a noticeable difference between the NOGAPS run and the COAMPS run. The area near Pt. Santa Cruz (a coastal headland area) displayed higher values with the COAMPS forcing (Figure 12) than with NOGAPS (Figure 13). Also, the oceanic front originating at the mouth of Monterey Bay was more distinguishable in COAMPS near Monterey Bay, but offshore NOGAPS gave a better interpretation of the frontal boundaries. The most distinguishable difference was located south of Monterey Bay along the Big Sur coastline. For NOGAPS the region extended further offshore and farther to the south than for COAMPS. Although the region covered was not as extensive with COAMPS, there were higher values of standard deviation localized within a region of a coastal headland. These plots suggest the higher resolution of the COAMPS wind field better captured the influence of the coastal features.

Annual averages of the surface velocity vectors were computed for both the COAMPS (Figure 14) and NOGAPS (Figure 15) fields. A comparison between the two vector plots displayed a distinct offshore movement of water located adjacent to the Pt. Sur headland in the COAMPS run, while the NOGAPS run lacked the offshore movement of water. Also, in the northern upwelling location, near Pt. Santa Cruz, COAMPS displayed a much stronger southward movement of water than the NOGAPS run.

The comparison of the standard deviation between the COAMPS U and V velocity vectors (Figure 16) and NOGAPS U and V velocity vectors (Figure 17) revealed some significant differences. The first comparison done was between the U velocity vectors. As seen in Figures 16 and 17, the COAMPS run has a much higher overall standard deviation throughout the model domain. For one area, north of Monterey Bay, COAMPS has a much higher fluctuation of surface velocity in the east/west direction. Within the Monterey Bay, in the southern portion there is another local maxima near Monterey. Along the Big Sur coastline is the most significant difference between the two runs. The NOGAPS run shows very little fluctuation of east/west velocity while the COAMPS run shows a region of high fluctuation with a local maxima imbedded within the region. The COAMPS high intensity areas are grouped into local maxima, which commonly occur near coastal headlands, similar to that seen in the sea surface temperature fields. These local maxima are not displayed in the NOGAPS runs. Along the coast a line of low standard deviation values was sandwiched between the land and grid points that had a much higher standard deviation. It was determined that some boundary problems exist in both the NOGAPS and COAMPS runs.

In the comparison between the standard deviation of the V velocity vectors the same boundary problems were evident. The COAMPS forced V velocity vectors displayed two regions of high fluctuation which had local maxima within them. The first was north of Monterey Bay, similar in location to the area in the U velocity plot (Figure 16), with the local maximum on the north side of the headland. The second area stretches from the tip of the Monterey Peninsula to the south along the coast with the local maximum located near the Pt. Sur headland. The NOGAPS results showed very little fluctuation throughout the domain.

C. SEASONAL DATA

The observed winds from the M3 buoy, which was located outside of the mouth of Monterey Bay, were used to identify time frames that were favorable for upwelling events (Figure 18). The year was broken down into four separate seasons. Season 1 is days 1 – 90, Season 2 is days 91 – 180, Season 3 is days 181 – 270, and Season 4 is days 271 – 365. Seasons two and three show winds favorable for upwelling while seasons one and four show the influence of winter storms that occur along the California coastline. Because the wind direction changes so often and so rapidly those seasons are not favorable for upwelling events. The existence of wind reversals is significant in determining the onset and relaxation of an upwelling event. The duration of along coast winds is significant in determining the duration, area covered, and strength of an upwelling or downwelling signature. Upwelling favorable winds are winds that are blowing in the southeast direction and are parallel to the coast. This, combined with the Coriolis force, causes the surface waters to be pushed away from the coast to be replaced with the cooler, nutrient rich water from below.

Seasonal averages were computed for the sea surface temperature and the surface velocity vectors. The seasonal means of sea surface temperature gave an indication as to what time of year the cooler sea surface temperatures were present. In both COAMPS (Figure 19) and NOGAPS (Figure 20), the coolest sea surface temperatures were during season 2, while the other three seasons contained a large amount of warm water influx from the south. This warm water influx is due to the one way coupling with the PWC model and advects more warm water into the model domain than what occurs in nature. NOGAPS had a larger amount of warm water influx and it propagated further to the north, which served to mask the upwelling events that occurred at the southern and northern upwelling locations. Because the influx of warm water from the south did not penetrate as far north in the COAMPS run (Figure 19), the northern upwelling location can be characterized by the cooler mean temperatures at the coast.

The seasonal means for surface velocity vectors were plotted and compared. When looking at the COAMPS surface velocity seasonal averages (Figure 21), a strong westward movement of water can be seen adjacent to the Pt. Sur headland as well as a

strong southward movement of water away from land near the northern coast of Monterey Bay, near the Pt. Santa Cruz location. This corresponds to the off-shore movement of water related to coastal upwelling. The seasonal averages closely relate to the annual wind plot (Figure 18) in that season one showed neither as strong an upwelling signature nor a high amount of water movement to the south. The seasonal average for the fourth season showed a slight onshore flow, more than season two and three. This was caused by the influence of Pacific storms inhibiting the development of upwelling events. In seasons two and three there was a strong southward movement of water north of Pt. Sur, which corresponded to the along coast winds pushing the water to the south, while Coriolis pushed the water away from the coast, as mentioned above.

The NOGAPS seasonal surface velocity (Figure 22) did not show a localized maximum of westward water movement as was observed in the COAMPS case. The along shore flow was present, strongest in seasons two and three, but there was very little offshore flow. Instead of upwelling along the coast, the values correlated to downwelling with the exception of season one. The strongest downwelling signature was visible along the Big Sur coastline, while the Pt. Santa Cruz area continued to display upwelling favorable characteristics. In the Pt. Sur area there was an area of maximum surface currents, but the intensity of southward moving water was much less than in the COAMPS case.

D. REMOVING THE SEASONAL CYCLE – HIGHPASS DATA

The standard deviation plots plainly outlined the two primary locations where upwelling was present. These areas of high variability were due to large fluctuations of temperature and water movement. From any grid point in the model domain it was possible to compute the time series of temperature fluctuation (Figure 23). In these figures the sea surface temperature fluctuation was plotted from both the NOGAPS (black) and COAMPS (red) runs. Grid point 2806 was located in the vicinity of Pt. Sur, while grid point 627 was an arbitrary point which was well offshore. The purpose of including the offshore time series is to illustrate the existence of a seasonal cycle at both grid points. The seasonal cycle was clearly outlined by the overall curve of the time series. The time series from point 2806 does not plainly identify the length of upwelling,

although it does show how often and dramatically the sea surface temperature changes along the coast.

To identify upwelling an energy density spectrum of sea surface temperature (Figure 24) was computed to determine the frequency of energy peaks. The peak located in the gray area is the energy from the seasonal cycle. Gaps occurred in the 7 day and 21 day region with significant energy peaks between them. These energy peaks were upwelling signatures. In order observe the actual temperature fluctuation caused by upwelling it was necessary to remove the seasonal cycle, leaving only the temperature fluctuations that dealt with upwelling. To do this a low pass filter was created. The low pass filter removed temperature oscillations that were greater than 90 days. The low frequency data was then subtracted from the original data set leaving behind only the high frequency temperature data that was desired.

Using the data after it had been filtered allowed examination of the model domain without the influence of the seasonal cycle. With the high pass data calculations were repeated to determine what was actually being influenced by the upwelling in the region. The standard deviation was recomputed, in both NOGAPS and COAMPS, and plotted. Again the year was broken down into four separate seasons; winter (days 1-90), spring (days 91-180), summer (days 181-270), and fall (days 271-365). COAMPS results (Figure 25) were again compared to the NOGAPS (Figure 26).

The winter season had two dramatic differences between the two runs. For COAMPS, a region of very high variance occurred along the Big Sur coast which correlated well with the upwelling region, but the region was constrained to one or two grid points along the shore. During the winter season there were numerous storms that could cause the area of high variability to be contained in such a small region, primarily due to the frequent wind direction changes within a short time period. In the same area along the coast in the NOGAPS run, there was a slightly higher variance in temperature than the surrounding area, but nothing as significant as the COAMPS run.

A seasonal feature in the NOGAPS run that was much more plainly seen than in the COAMPS run was a region of high temperature variability surrounded by areas of

lower temperature variability. This area could be identified as a boundary between the cold water from the north which is flowing south, and the warmer water that is being brought into the model from the south. In the filtered data, this boundary area is completely identifiable in each run, though in the NOGAPS run it is clearly defined. In the spring season this boundary region begins to break down in the NOGAPS run while in the COAMPS run it becomes more structured. The upwelling region along the Big Sur coast began to show higher values in each run and the region of high temperature variability began to spread further westward, consistent with the cold water transport off shore. The region of high temperature variability was more intense and covered a broader area in the COAMPS run than in the NOGAPS run. In the summer season the upwelling signature was still clearly seen in the COAMPS run although the region of westward water transport began to recede. In the NOGAPS run, there was no upwelling signature visible. In the COAMPS run there was a region beginning in the mouth of Monterey Bay that extended to the southwest. This was probably a region characterized by an oceanic front (Rosenfeld et. al. 1994, Paduan and Rosenfeld, 1996). This was also visible in the unfiltered standard deviation plots although it was partially visible in each run. In the filtered, high pass data it was plainly visible in the COAMPS run, but not in the NOGAPS run. In the fall season the upwelling signature was well established in each run, but the COAMPS run had higher intensities and the maximum values were centered around the Pt. Sur headland. The higher temperature variability extended to the south along the coast almost to the edge of the model domain. In all four seasons the first three rows of grid points along the southern boundary of the model seemed to have values equal to the minimum end of the scale. This was associated with difficulties associated with coupling the ICON model to the larger regional Pacific West Coast model.

E. UPWELLING CASE STUDY

The 9 km resolution wind fields provided by the COAMPS run produced more mesoscale features seen than the 100 km resolution wind fields from NOGAPS for all model results. The southern upwelling location centered around Pt. Sur displayed more dramatic upwelling signatures than the northern upwelling location. Because of these results the ICON model run using the COAMPS wind forcing was the model of choice

for a case study of a selected upwelling event. The case study took place from year day 80 (21 March) through 110 (20 April). Many of the mesoscale features can be seen in the case study. These features included upwelling, a cold water filament and a mesoscale eddy that formed in the southern portion of the model domain. Both the sea surface temperature field and the surface velocity vectors were useful in identifying the features.

The case study began with downwelling along the coast and warm water was concentrated along the coast (Figure 27). The winds shifted to upwelling favorable on day 85 and the resulting upwelled cold water was visible by day 87 (Figure 28). As the cold water upwelled, the interaction of the winds with Pt. Sur caused the cold water to be transported away from the coast in a cold water filament and form into an eddy. This process was seen in the sea surface temperature field (Figure 29).

The same features were seen in the surface velocity vectors (Figure 30). The concentration of the warm water along the coast was characterized by northward, on shore water movement. Upwelling was shown by strong southward, offshore water movement (Figure 31). The cold water filament extending offshore which fed the formation of an eddy was clearly seen as well (Figure 32).

The low pass data filter was applied for days within the case study and the results displayed even stronger signatures. The concentration of warm water along the coast was even more dramatic at the beginning of the event (Figure 33). Without the seasonal cycle present, the upwelling signature was even more intense than previously seen. The filtered data displayed a very strong upwelling signature which moved offshore to the northeast (Figure 34).

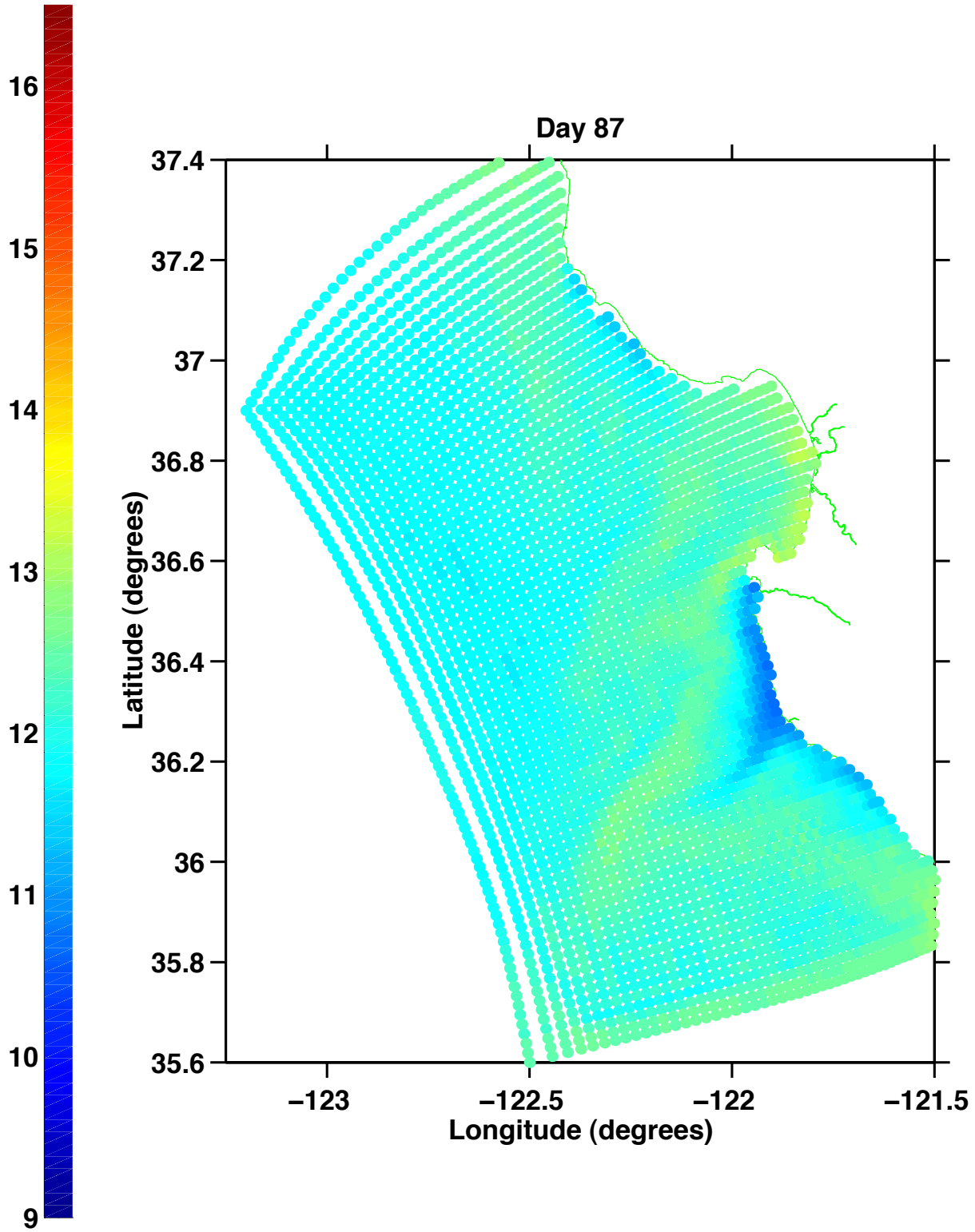

Figure 7. SST from COAMPS-forced ICON model run for day 87 (28 March) 1999 showing cold water upwelling near the coast.

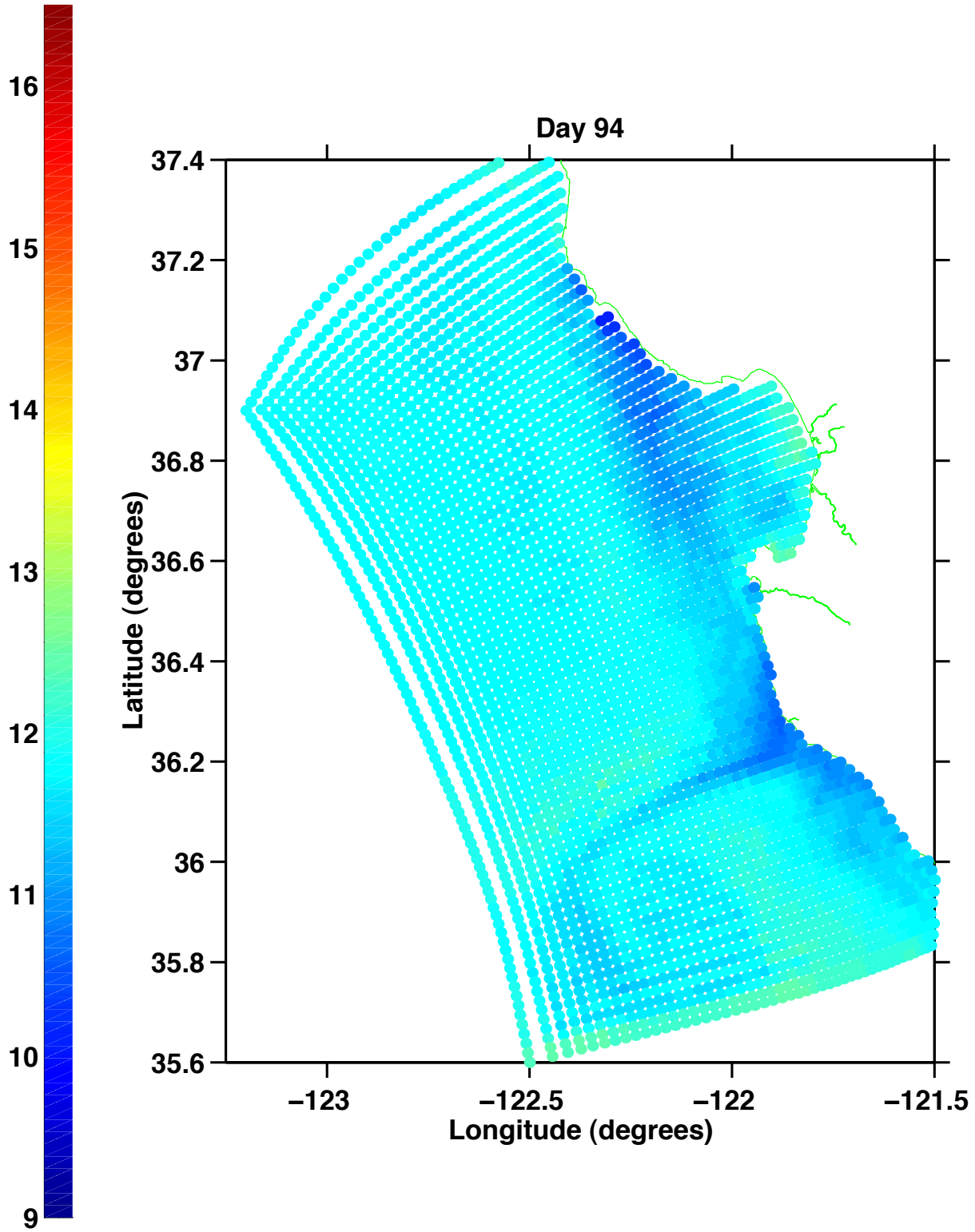

Figure 8. SST from COAMPS-forced ICON model run for day 94 (4 April) 1999 showing the presence of a cold water filament.

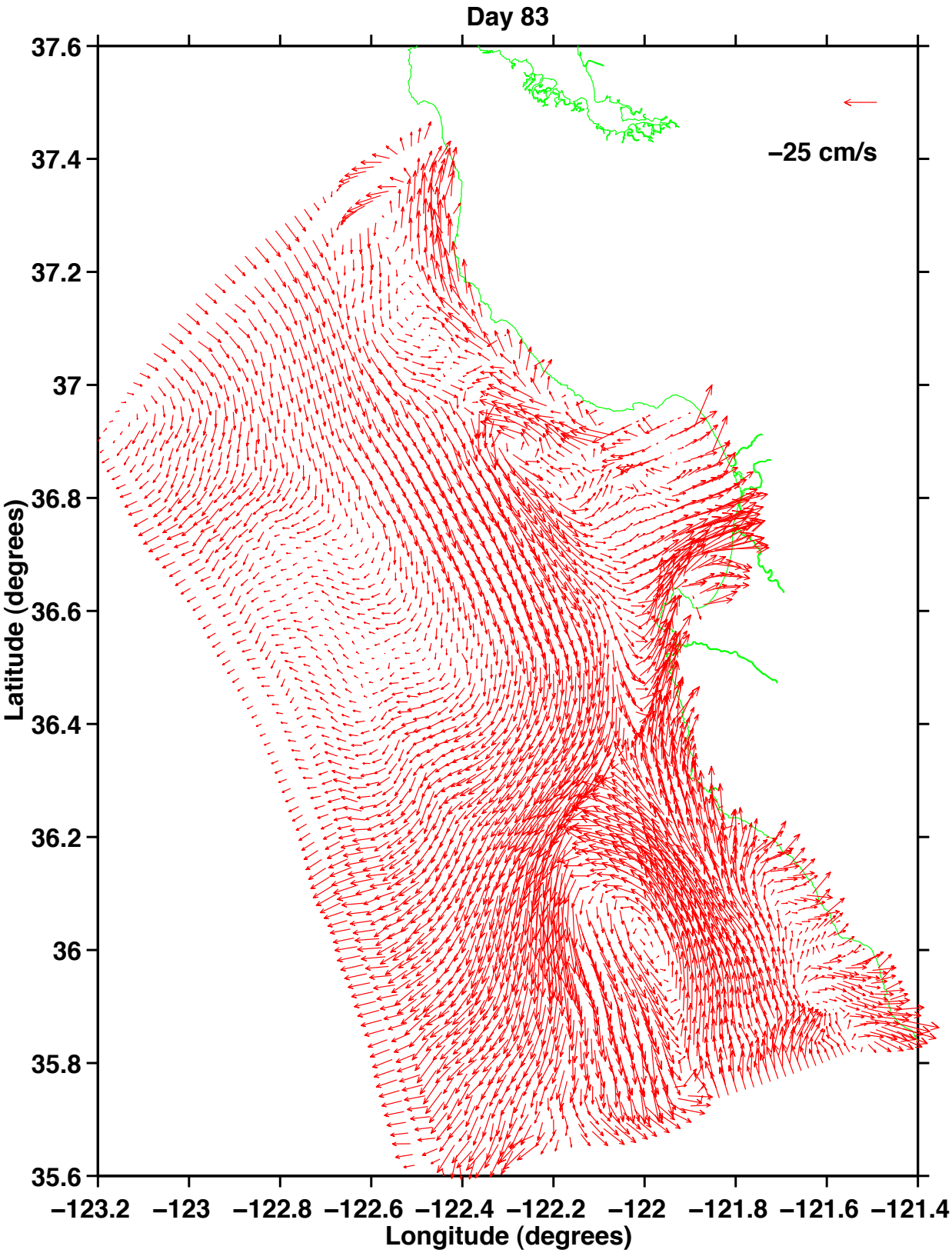

Figure 9. Surface velocity vectors from COAMPS-forced ICOON model run for day 83 (24 March) 1999 showing a mesoscale eddy near 36°N, 122°W.

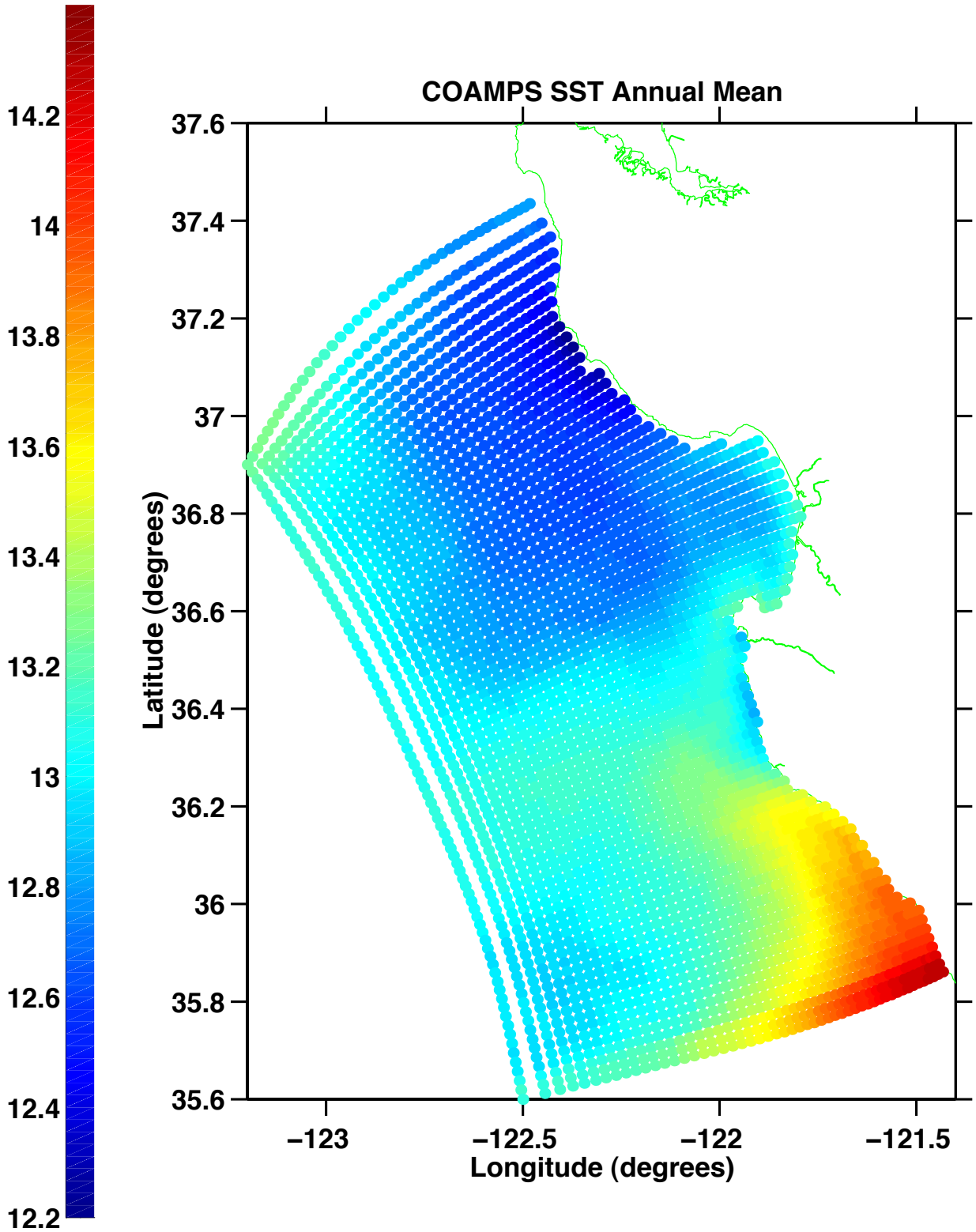

Figure 10. COAMPS-forced ICON model sea surface temperature average (annual).

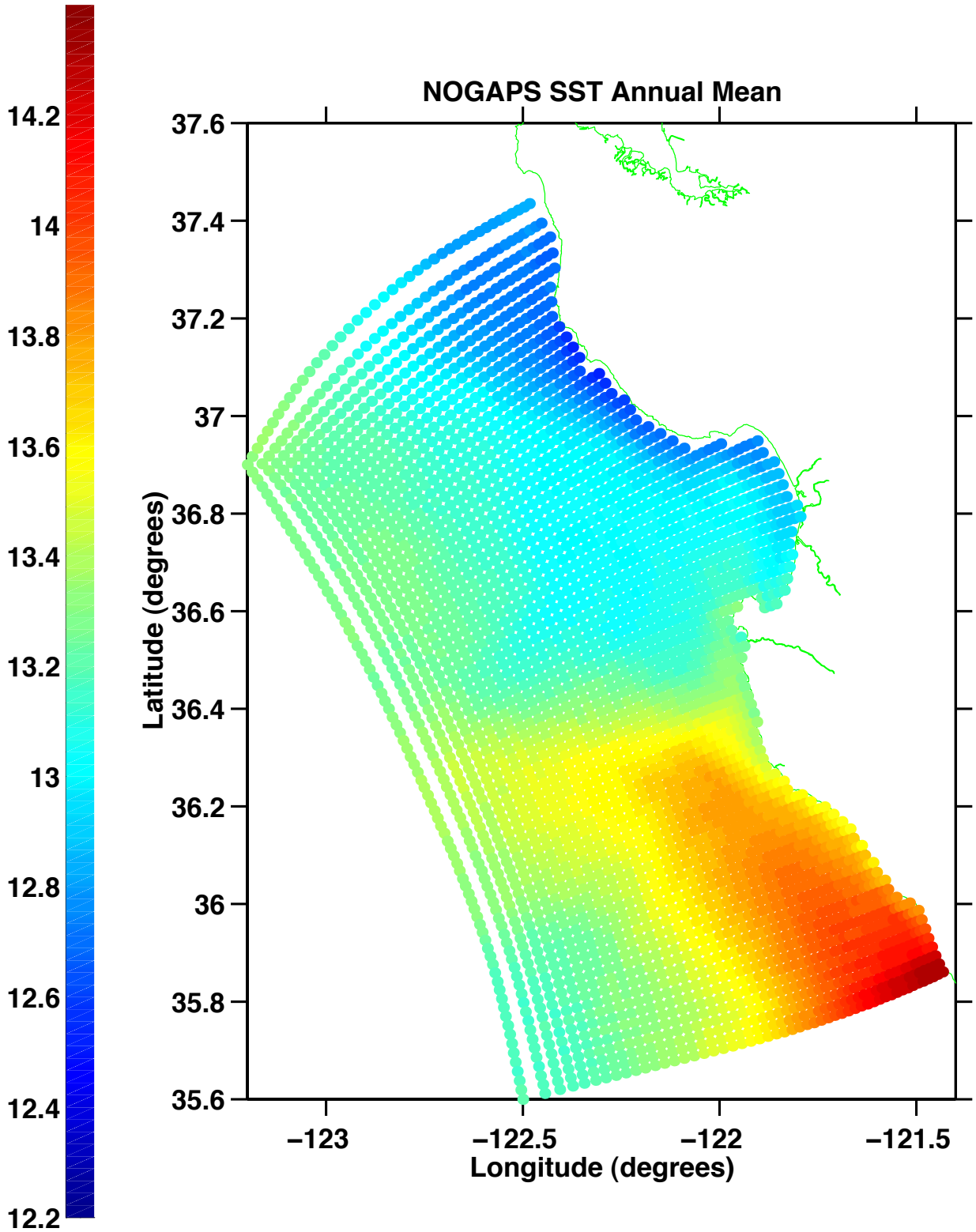

Figure 11. NOGAPS-forced ICON model sea surface temperature average (annual).

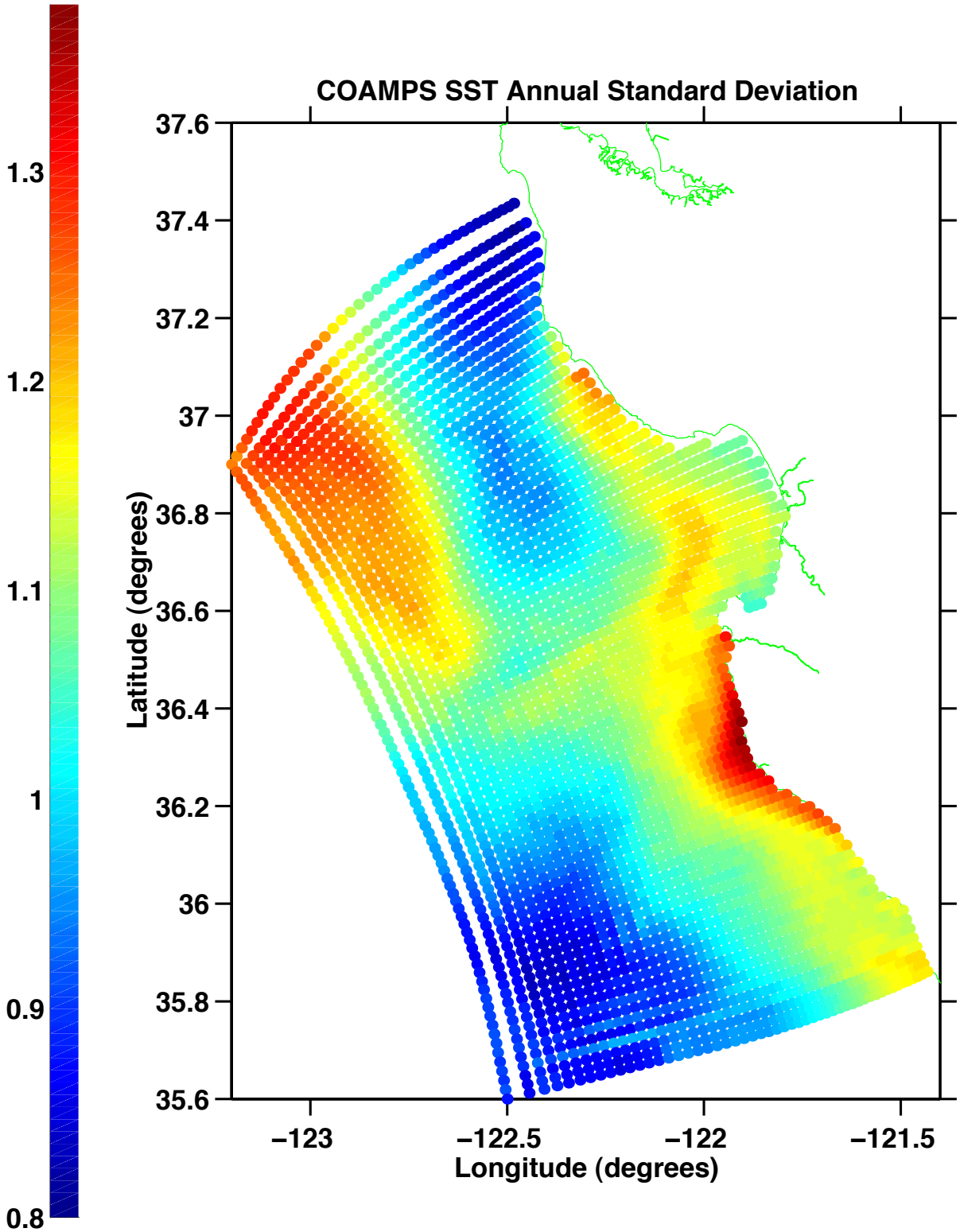

Figure 12. COAMPS-forced ICON model sea surface temperature standard deviation (annual).

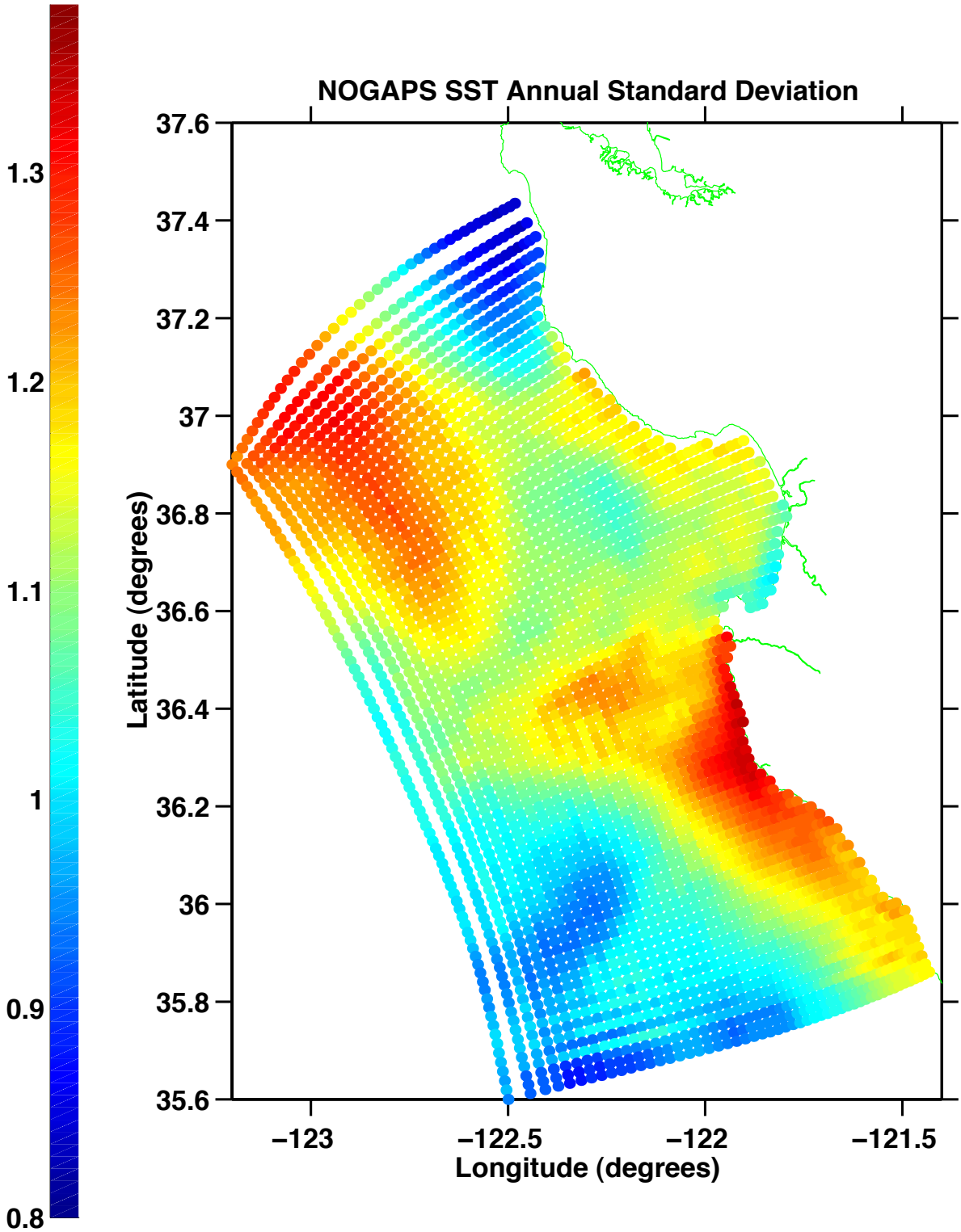

Figure 13. NOGAPS-forced ICON model sea surface temperature standard deviation (annual).

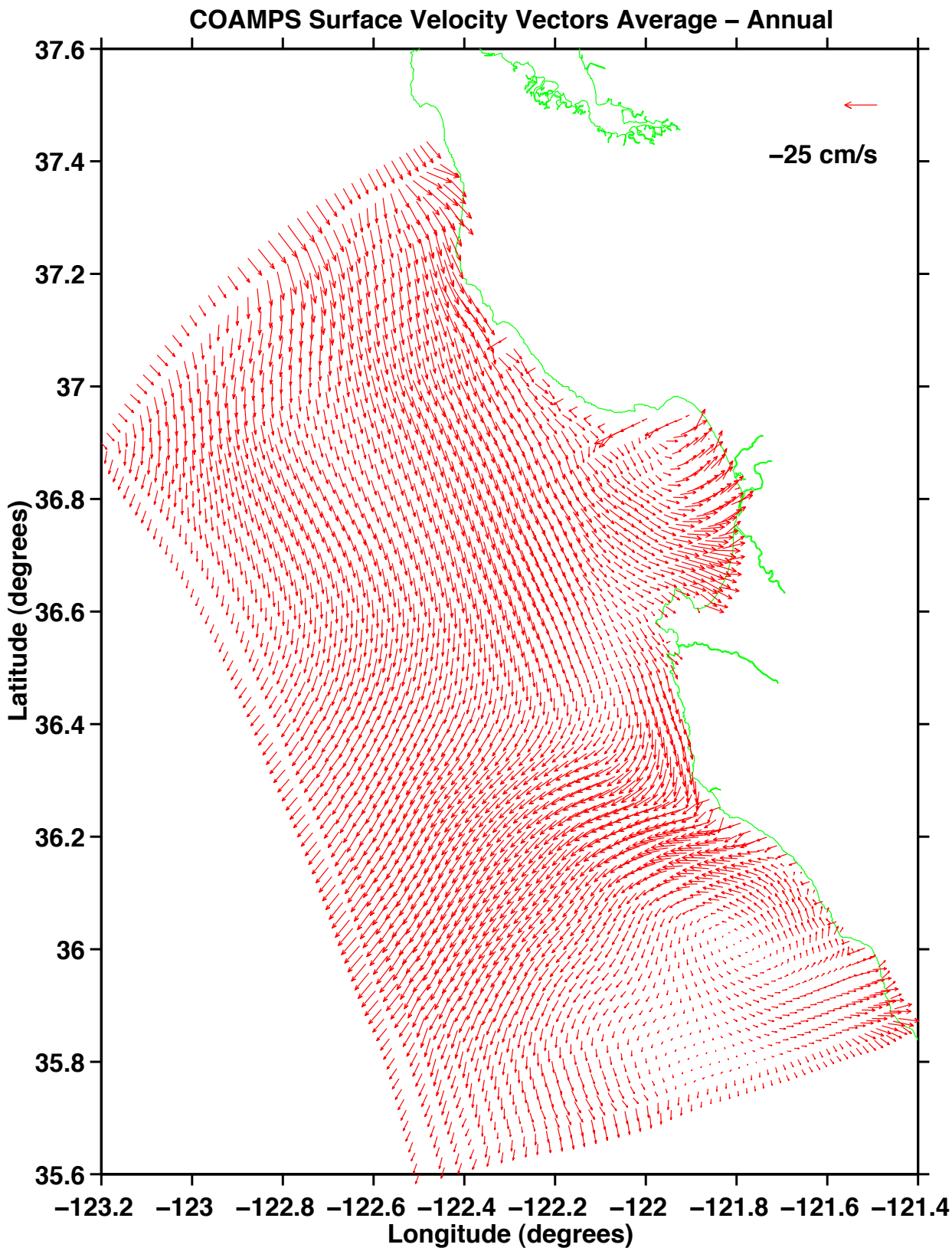

Figure 14. COAMPS-forced ICON model surface velocity vectors average (annual).

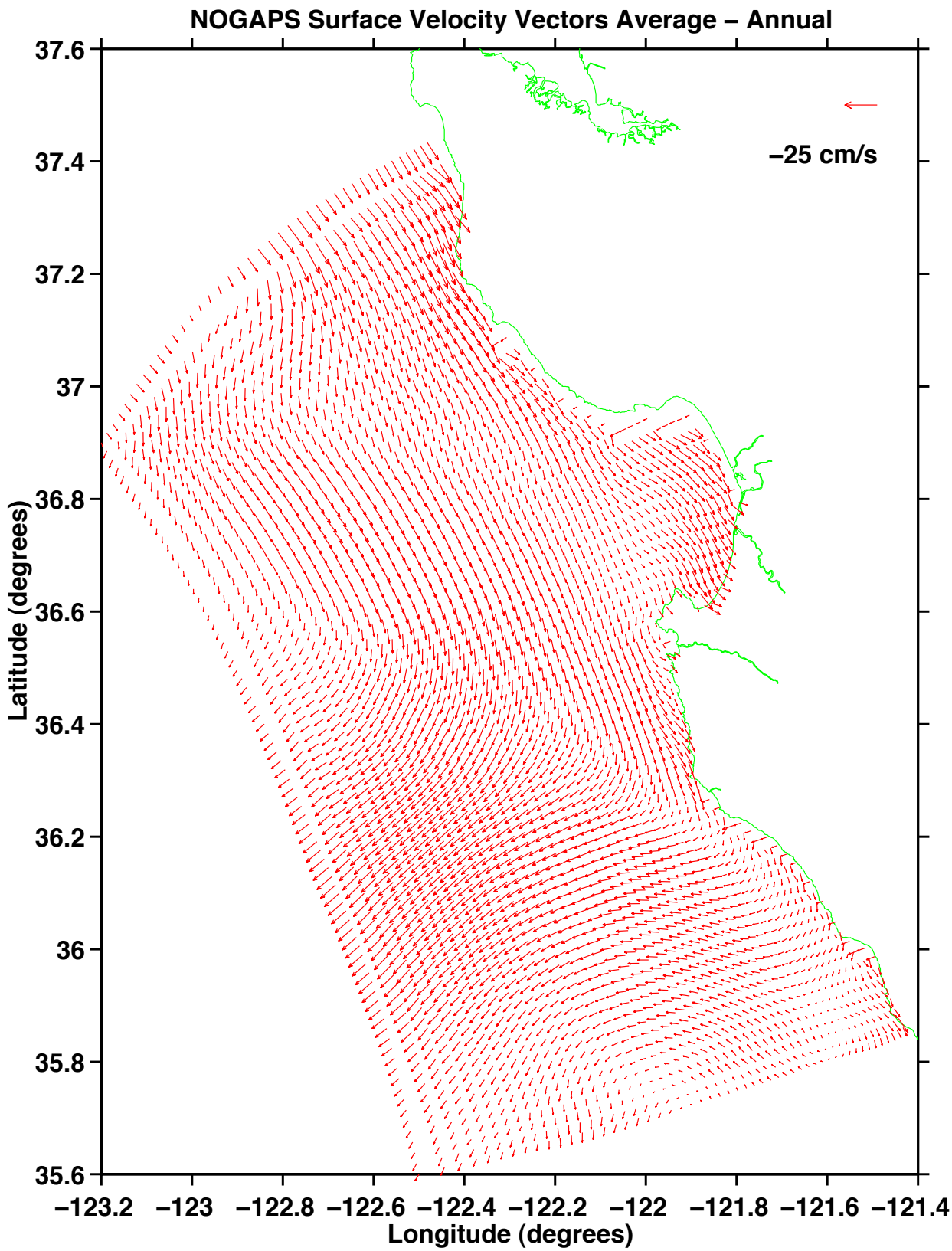

Figure 15. NOGAPS-forced ICON model surface velocity vectors average (annual).

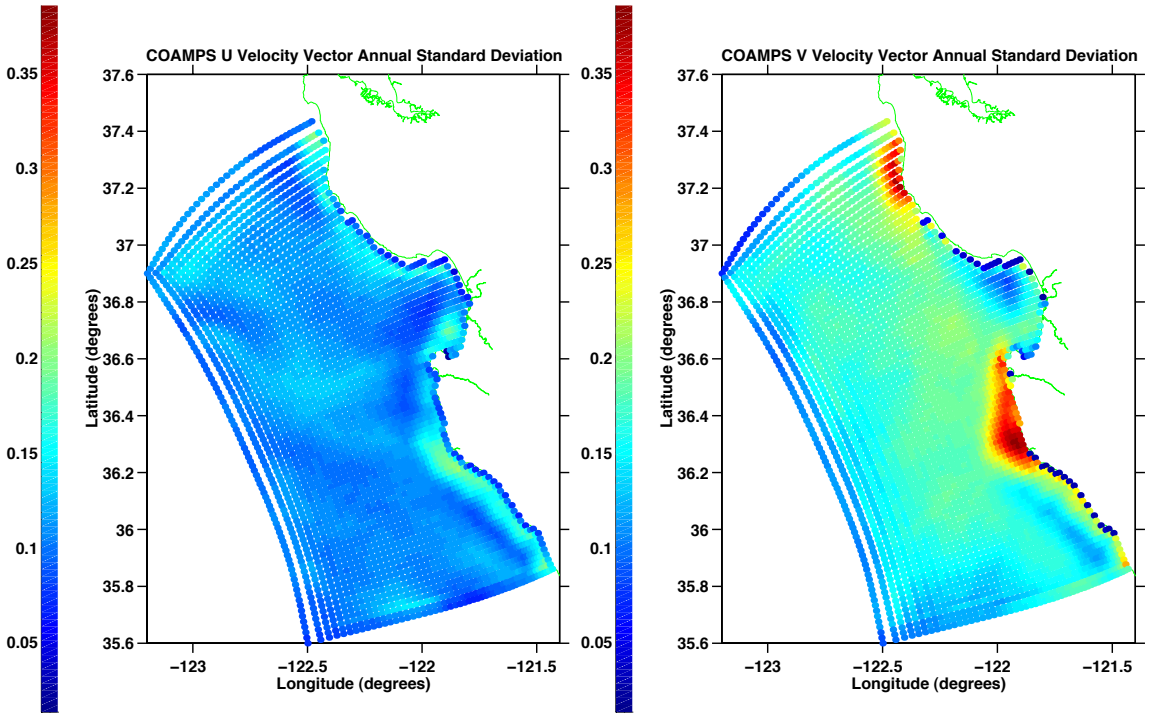

Figure 16. COAMPS-forced ICON model U and V surface velocity standard deviation (annual).

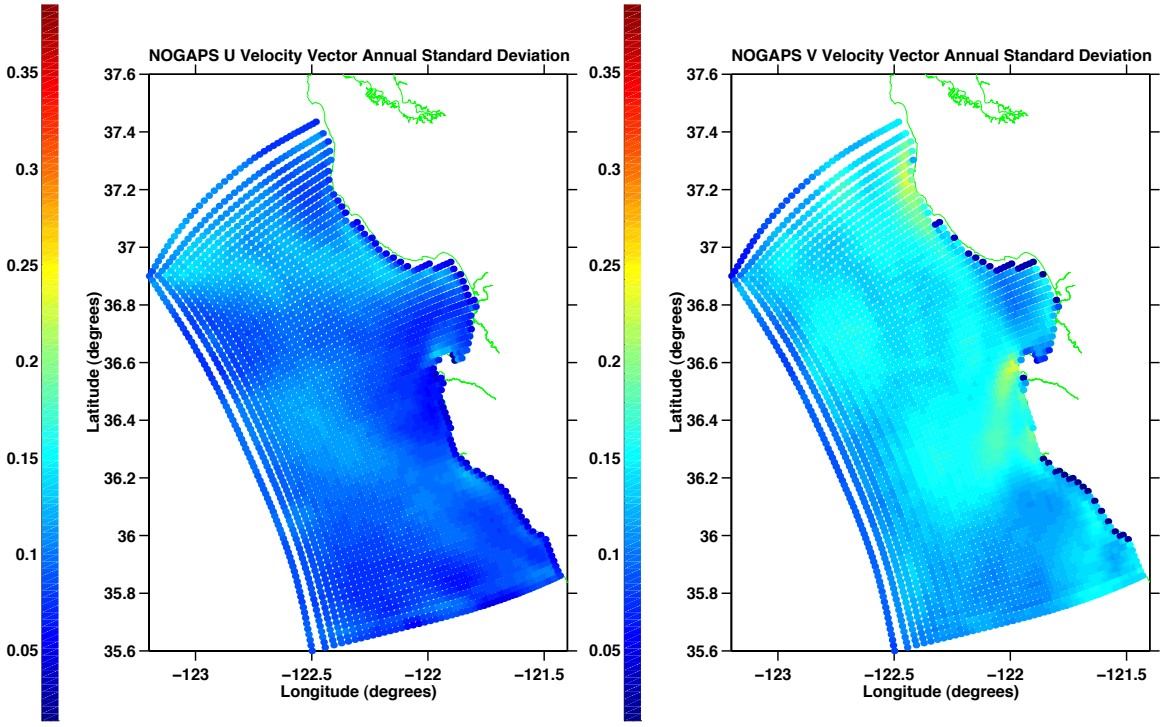

Figure 17. NOGAPS-forced ICON model U and V surface velocity standard deviation (annual).

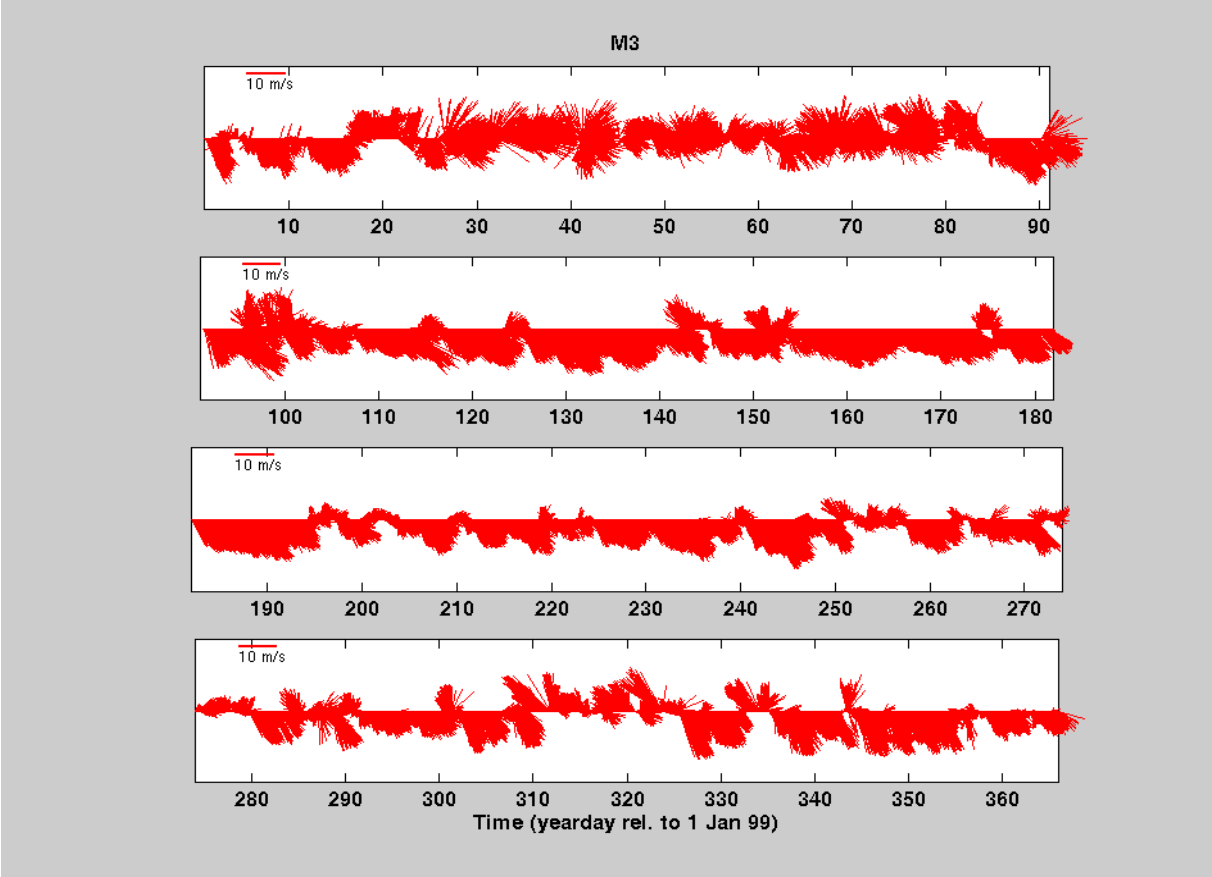

Figure 18. Observed surface winds at mooring site M3. The M3 wind sensors failed for days 194 to 202, so winds from M2 were used.

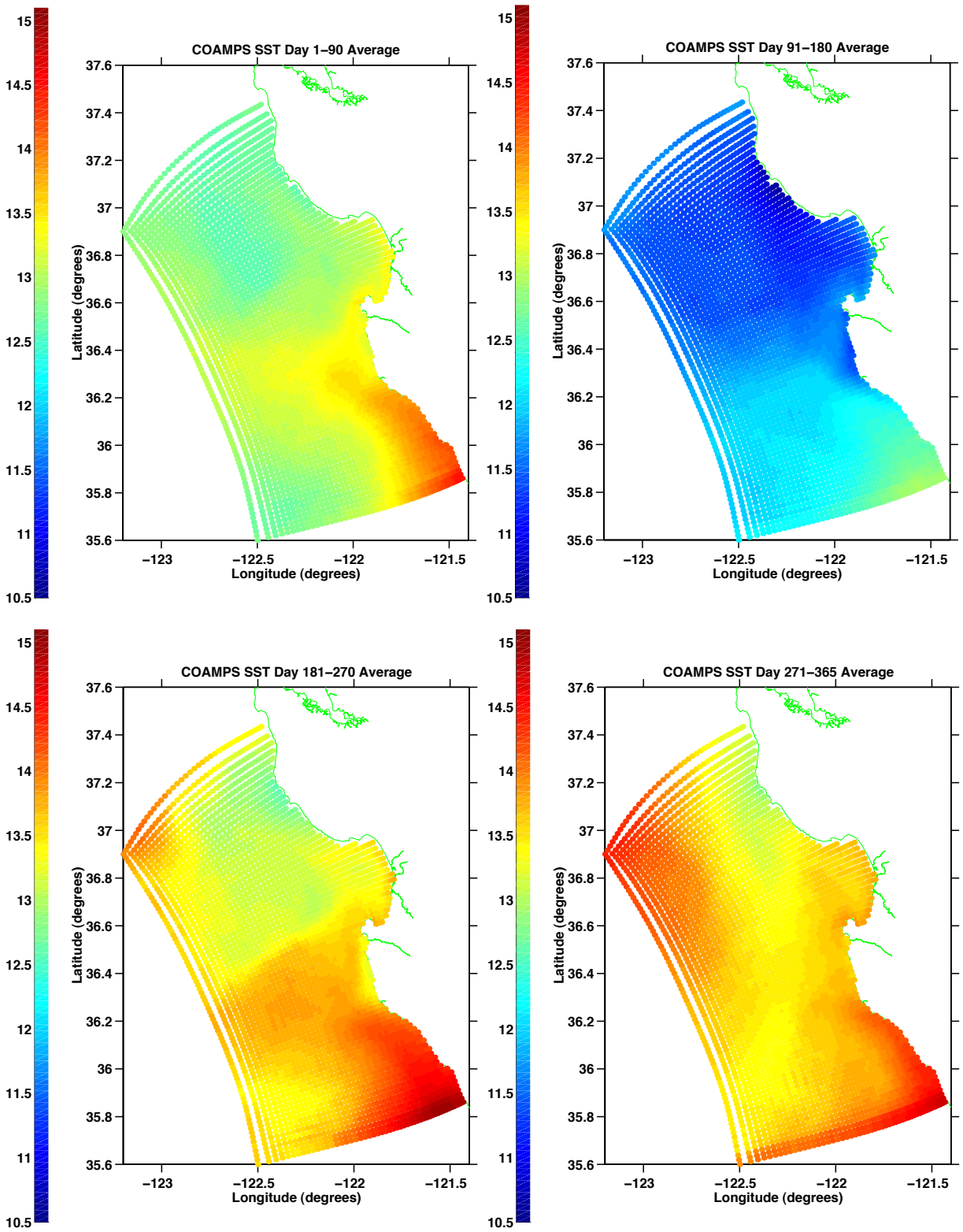

Figure 19. COAMPS-forced ICON model sea surface temperature average (seasonal).

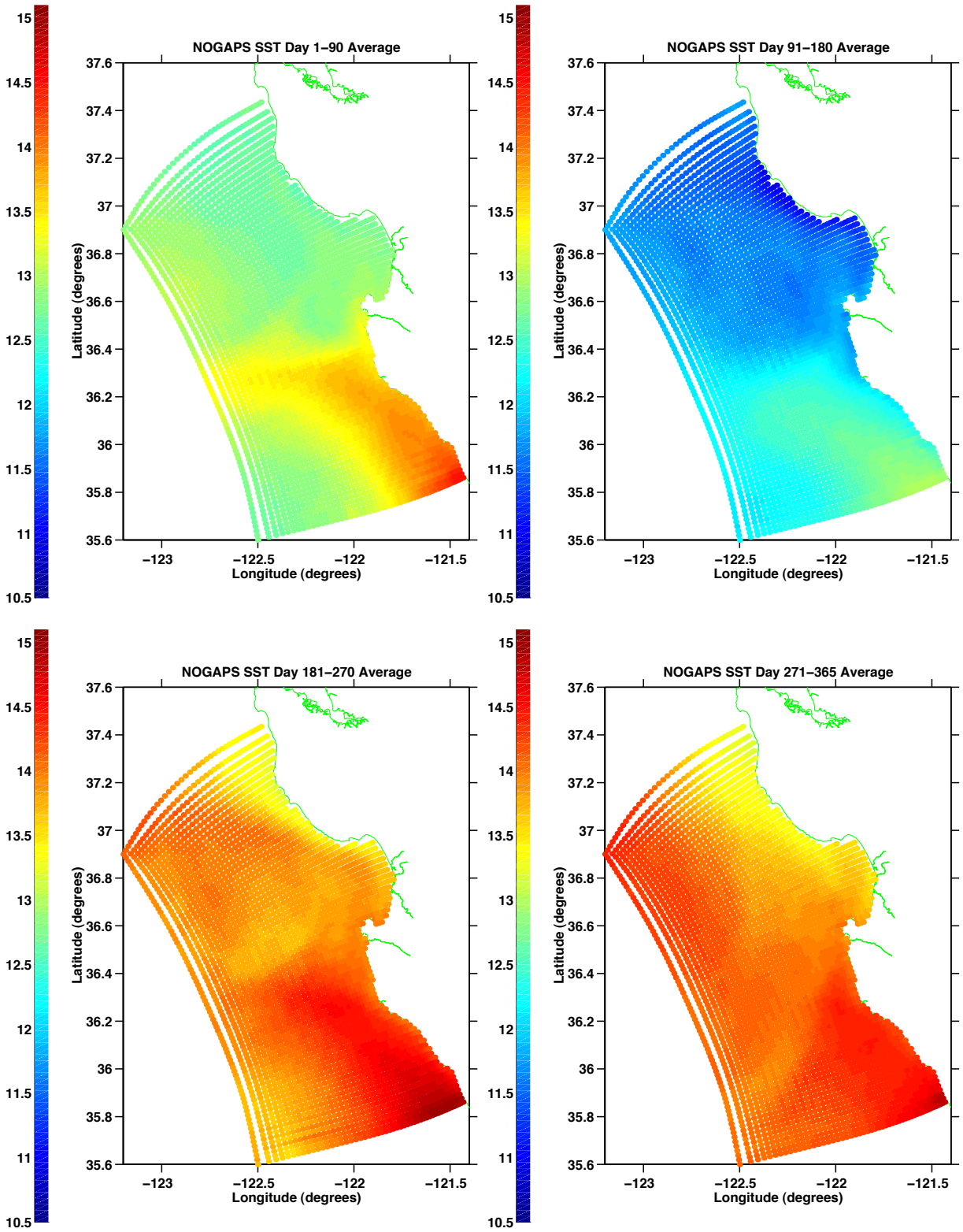

Figure 20. NOGAPS-forced ICON model sea surface temperature average (seasonal).

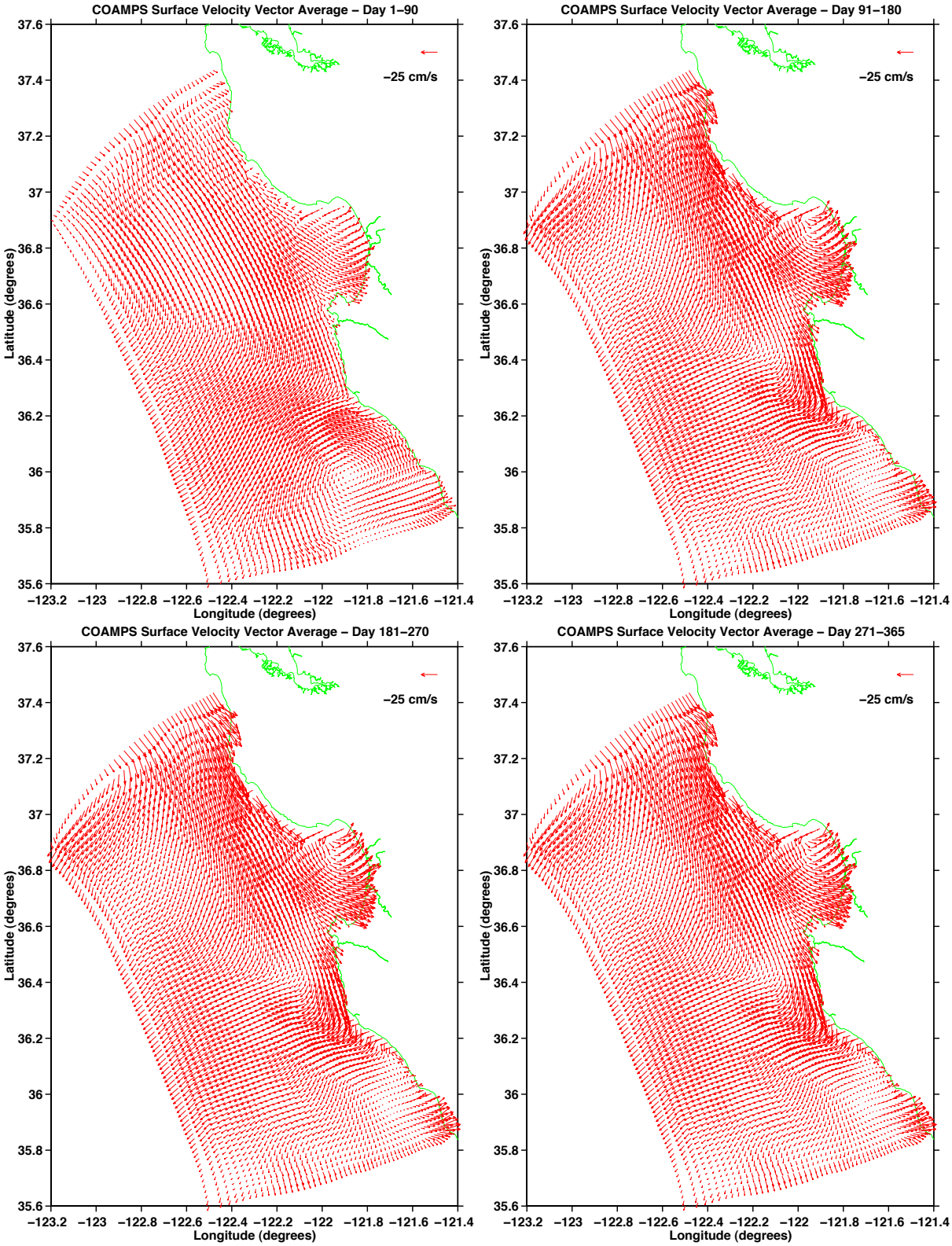

Figure 21. COAMPS-forced ICON model surface velocity vectors average (seasonal).

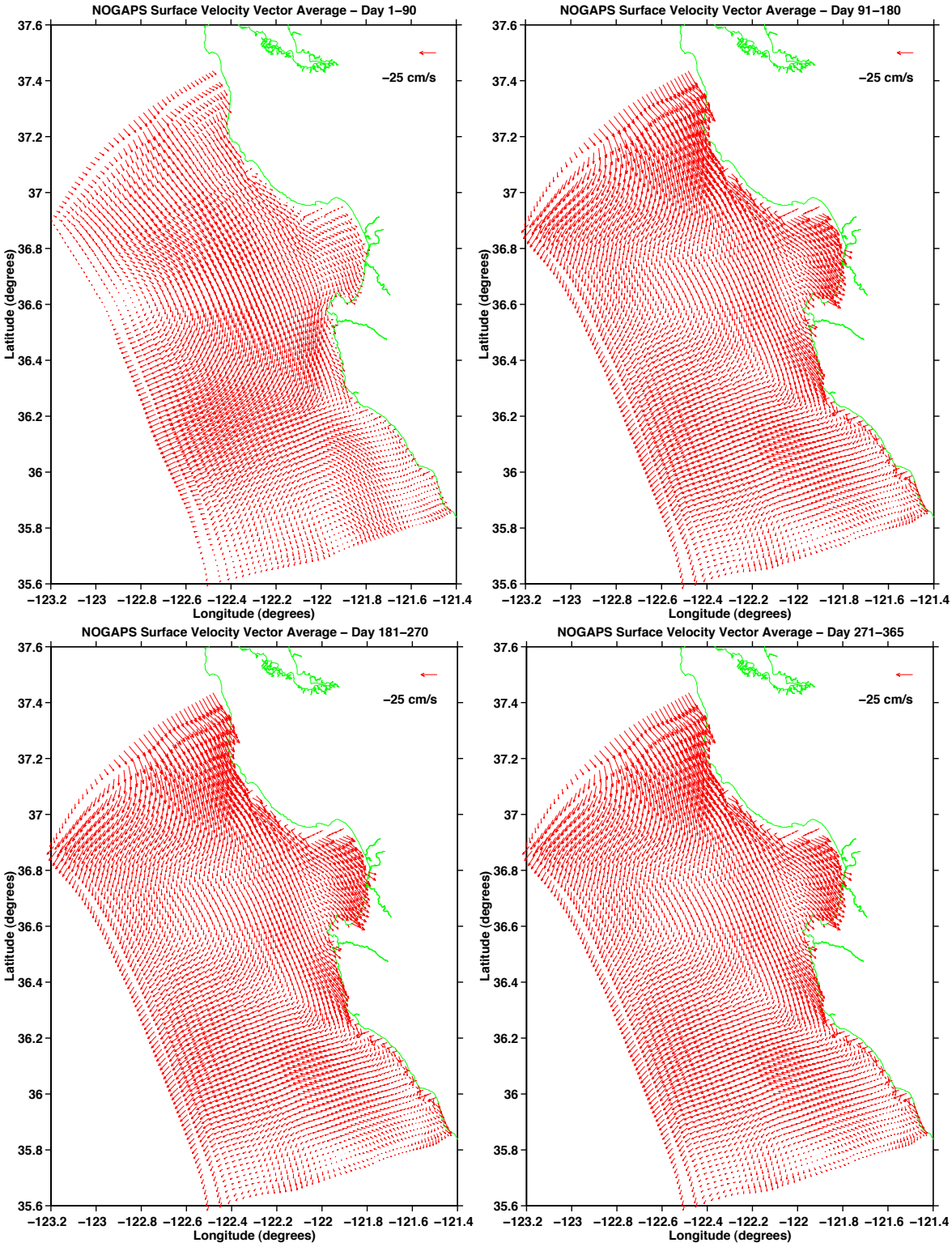

Figure 22. NOGAPS-forced ICON model surface velocity vectors average (seasonal).

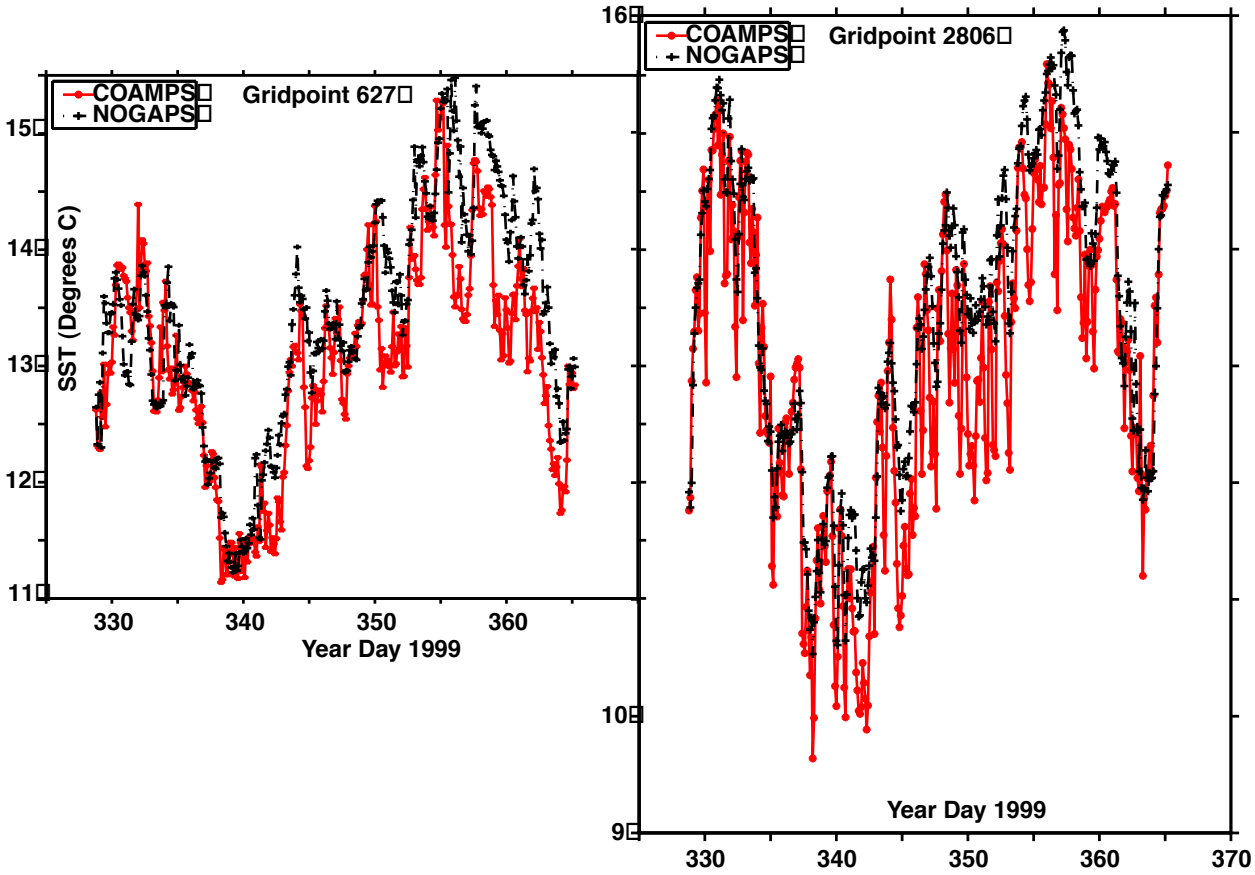

Figure 23. Fluctuation of SST at grid point 2806 and 627.

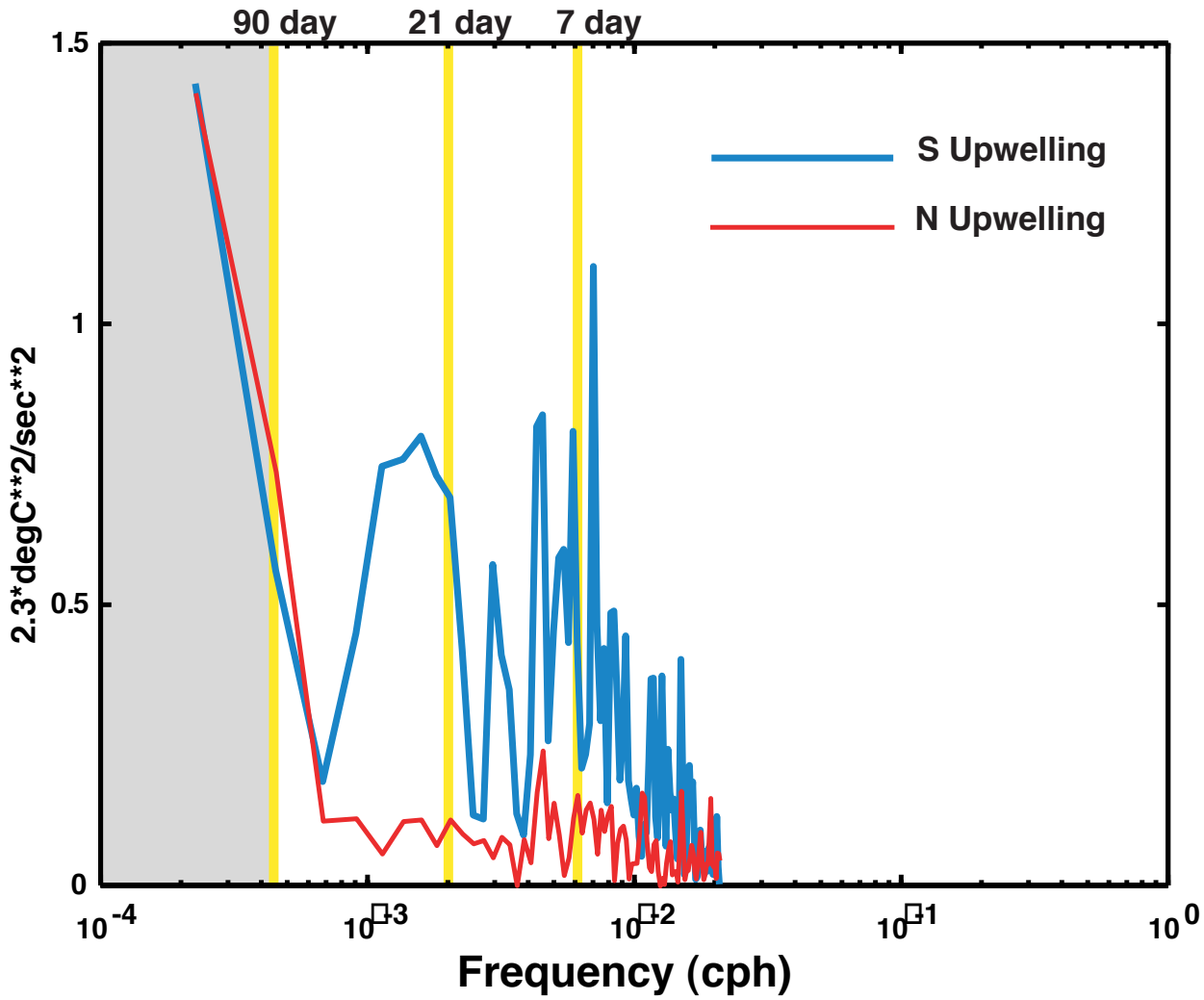

Figure 24. Energy density spectrum.

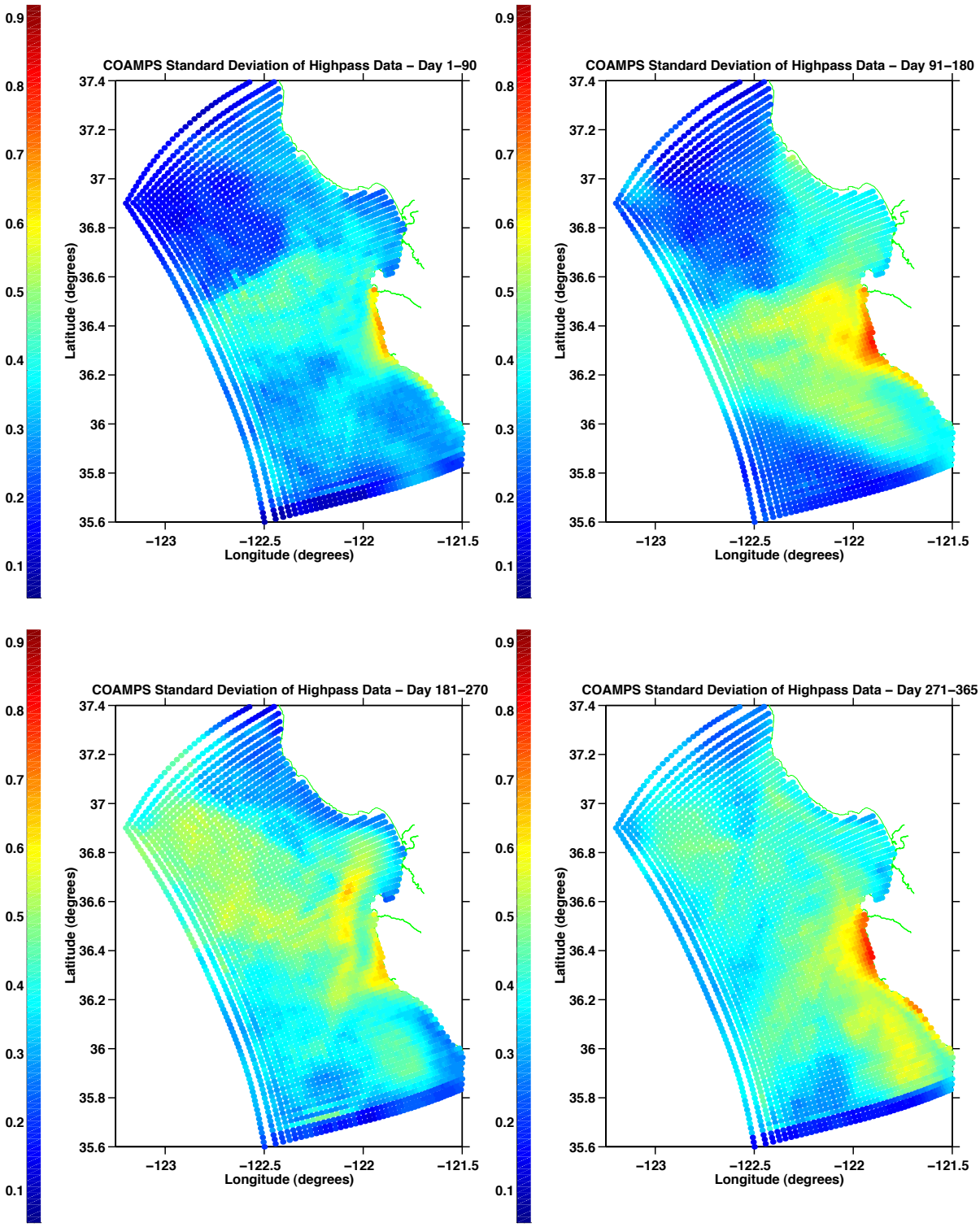

Figure 25. High pass filtered COAMPS-forced ICON model sea surface temperature standard deviation (seasonal).

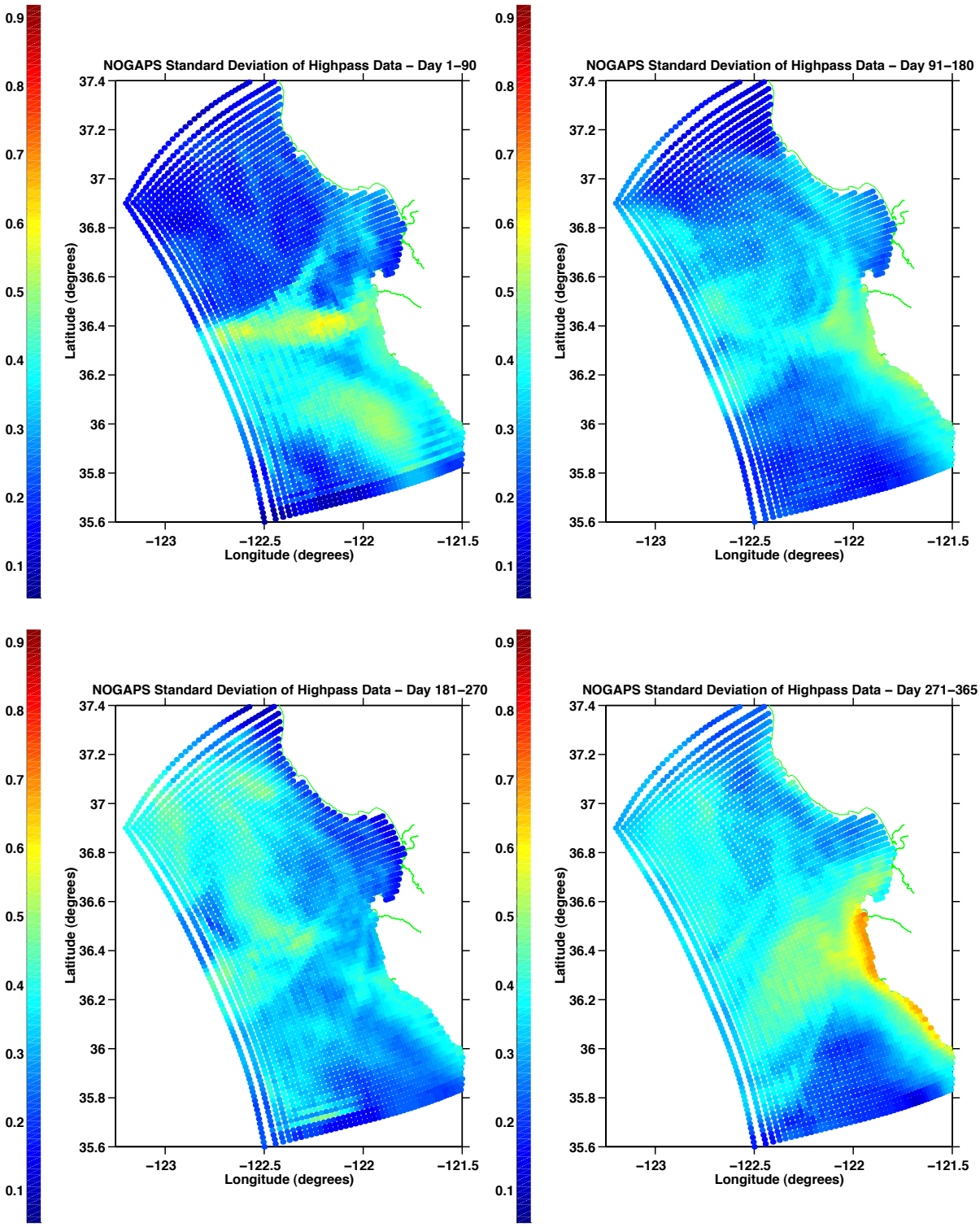

Figure 26. High pass filtered NOGAPS-forced ICON model sea surface temperature standard deviation (seasonal).

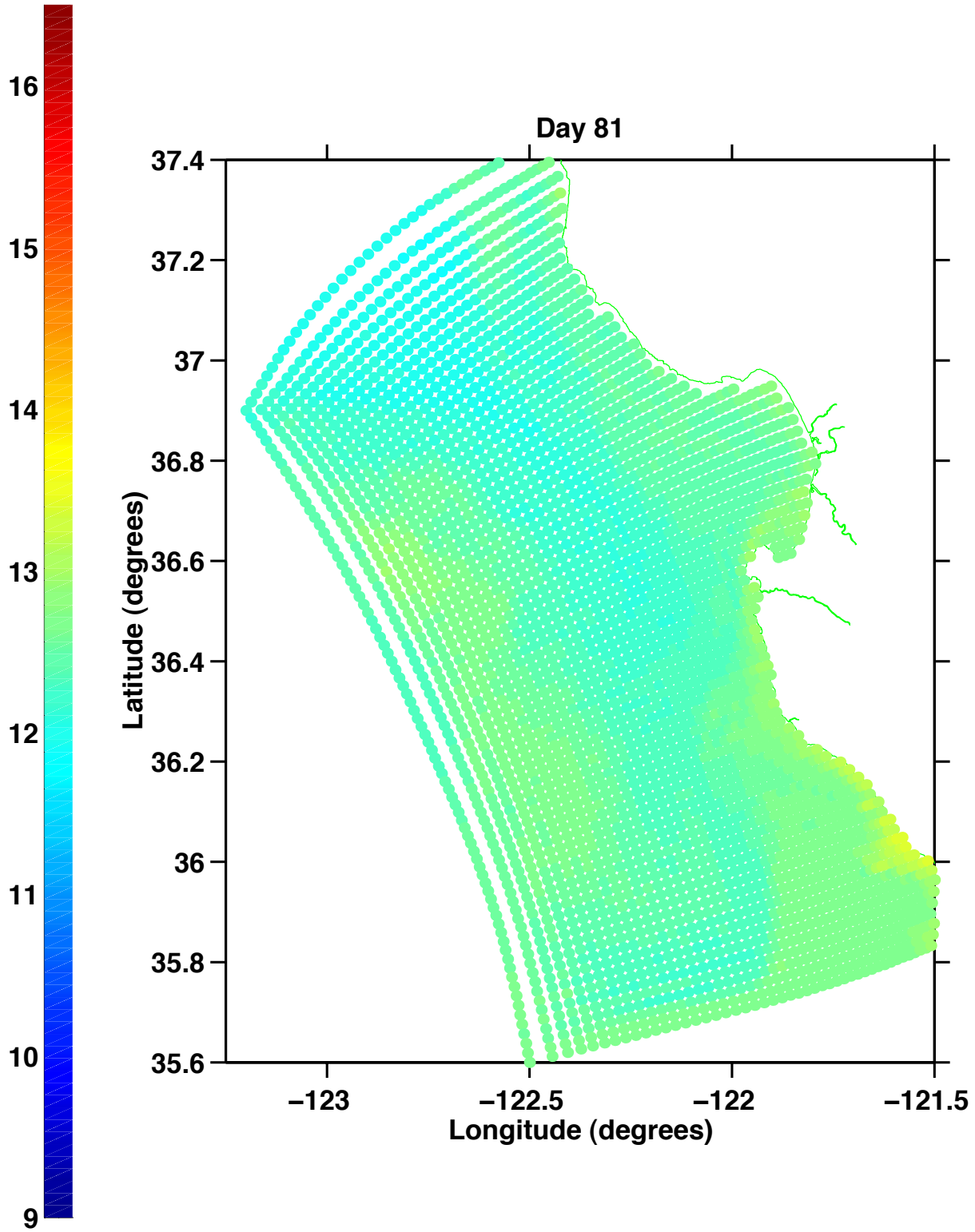

Figure 27. SST from COAMPS-forced ICON model run for day 81 (22 March) 1999 showing warm water concentration at the coast.

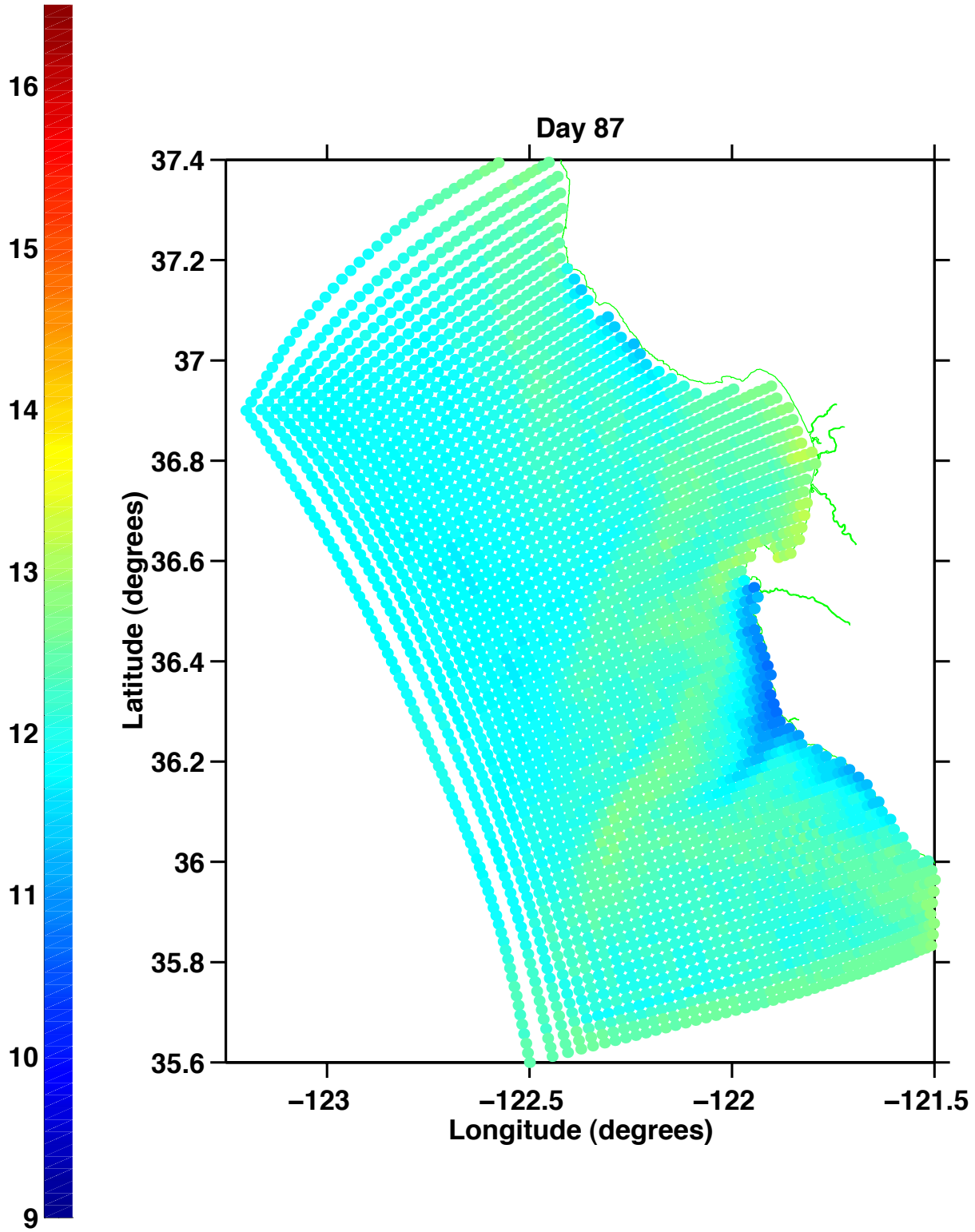

Figure 28. SST from COAMPS-forced ICON model run for day 87 (28 March) 1999 showing upwelling of cold water at Pt. Sur.

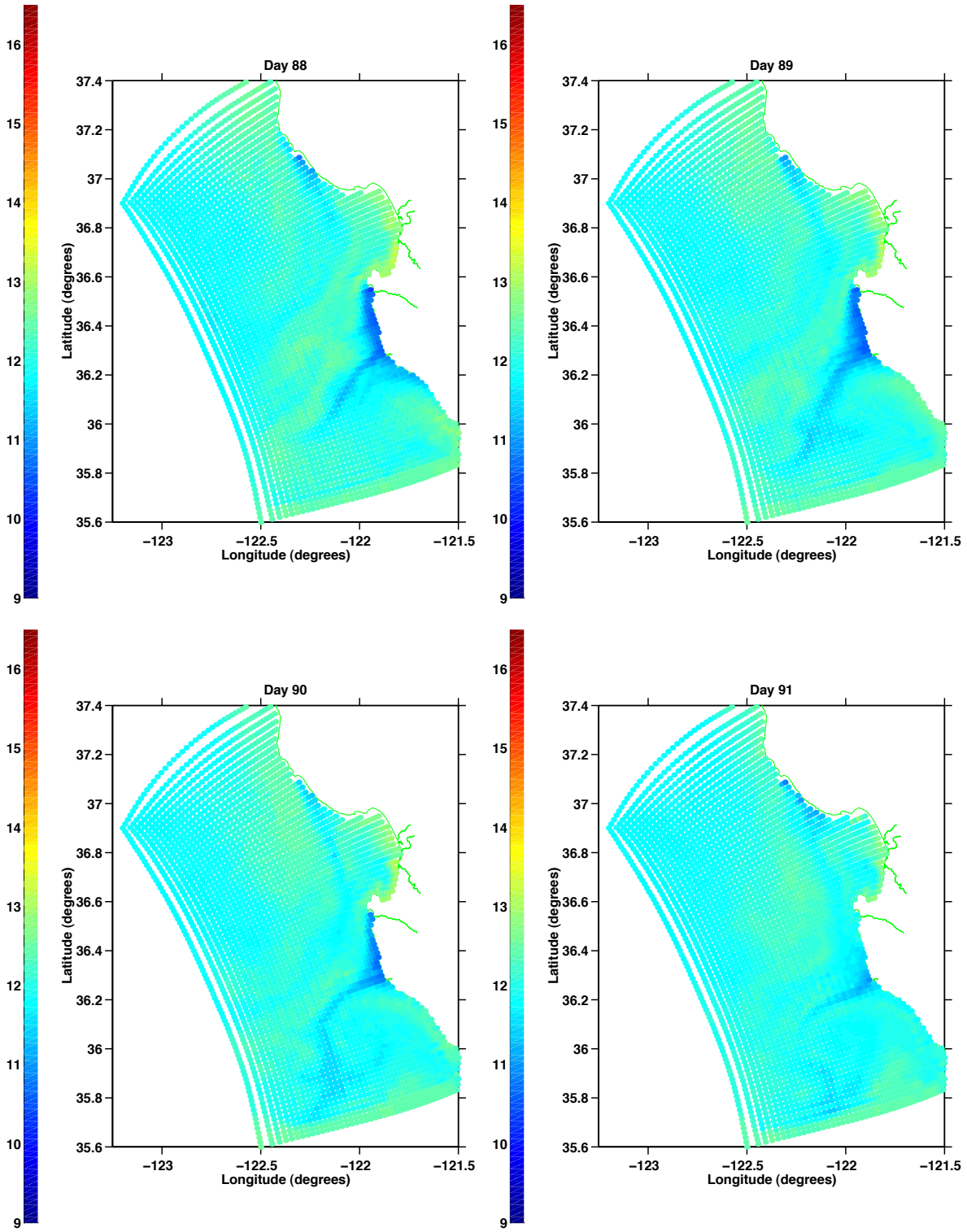

Figure 29. SST from COAMPS-forced ICON model run for days 88-91 (29 March – 2 April) 1999 showing filament and eddy formations.

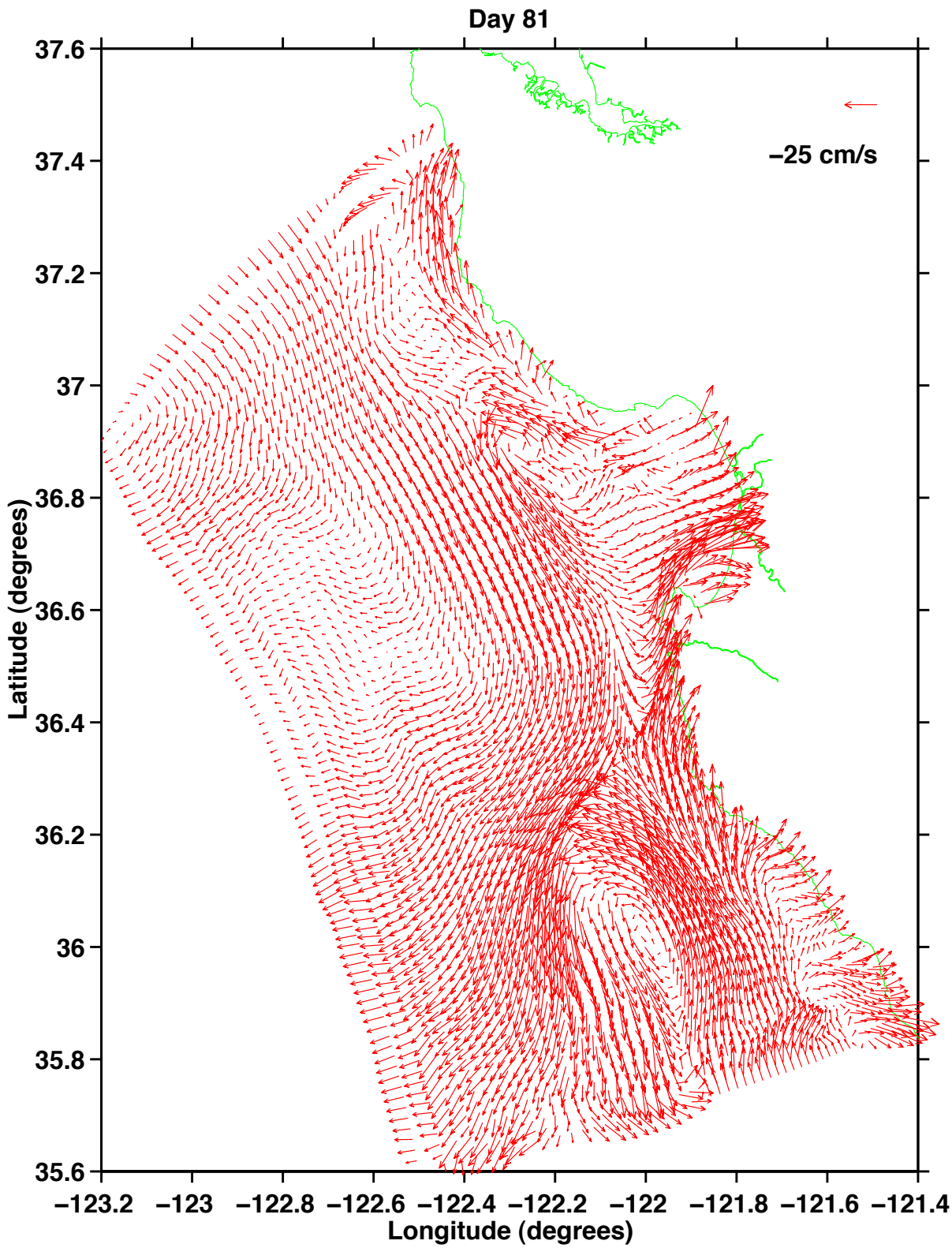

Figure 30. Surface velocity vectors from COAMPS-forced ICON model run for day 81 (22 March) 1999 showing concentration of warm water along coast.

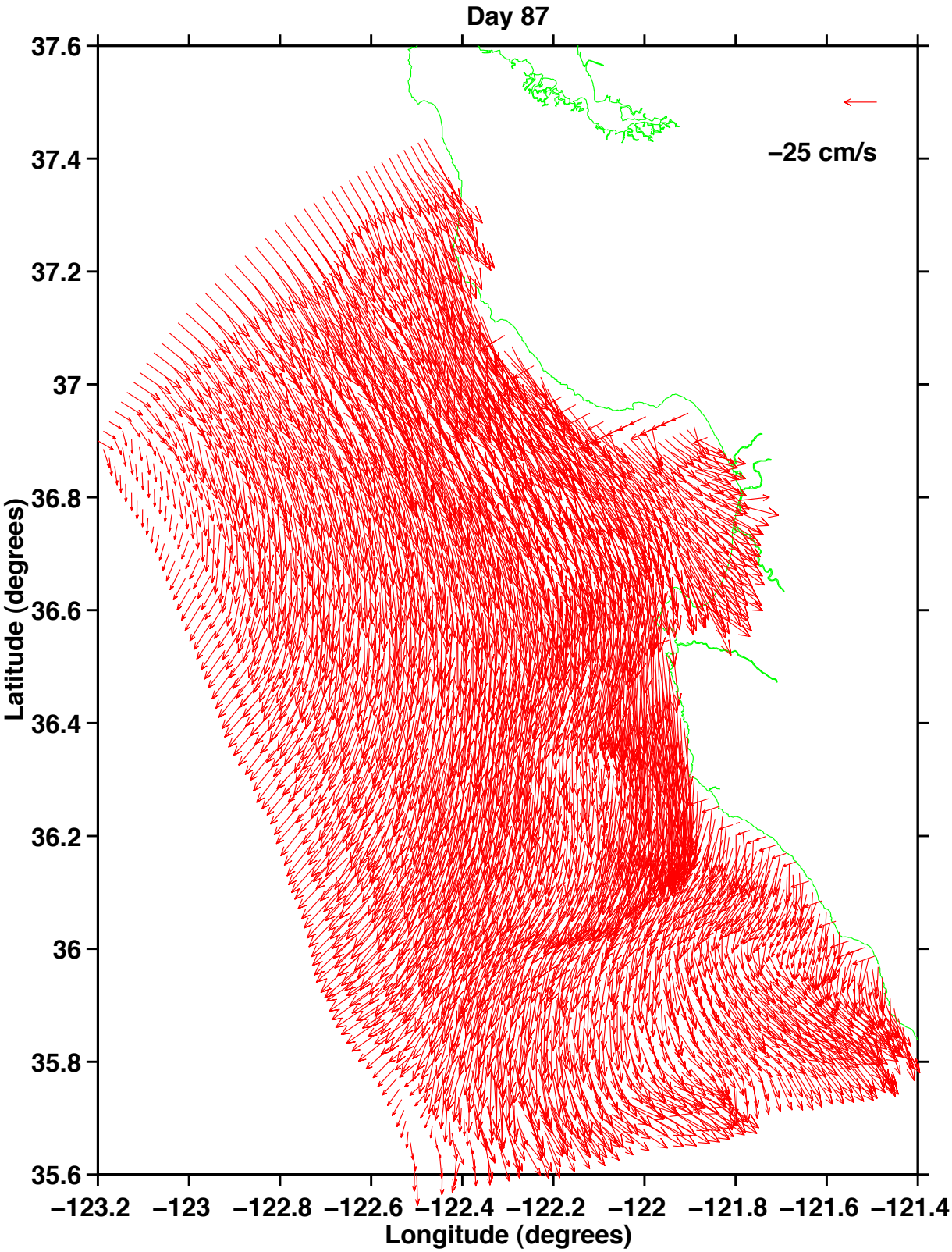

Figure 31. Surface velocity vectors from COAMPS-forced ICON model run for day 87 (28 March) 1999 showing upwelling of cold water at Pt. Sur.

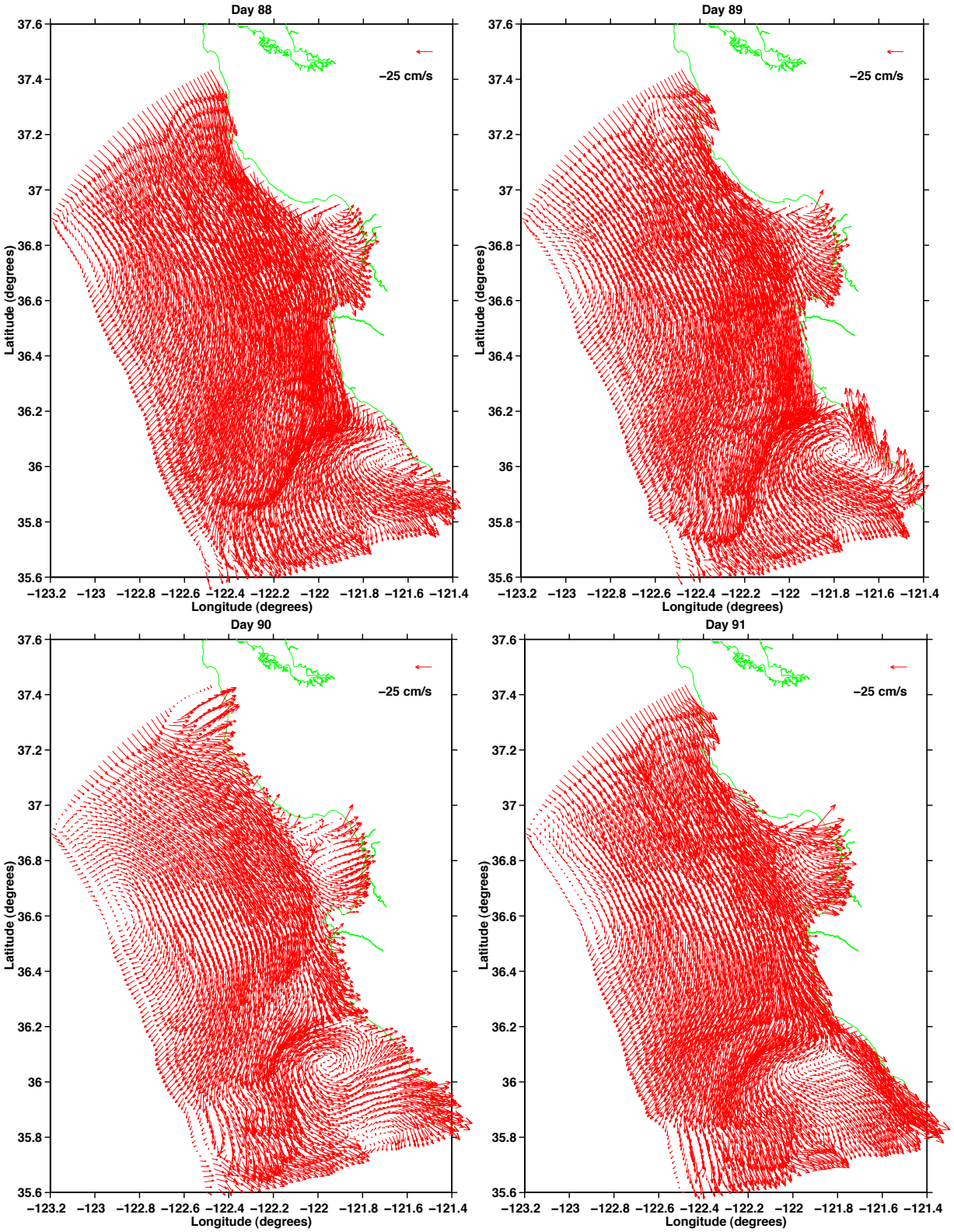

Figure 32. Surface velocity vectors from COAMPS-forced ICON model run for days 88-91 (29 March –2 April) 1999 showing filament and eddy formation.

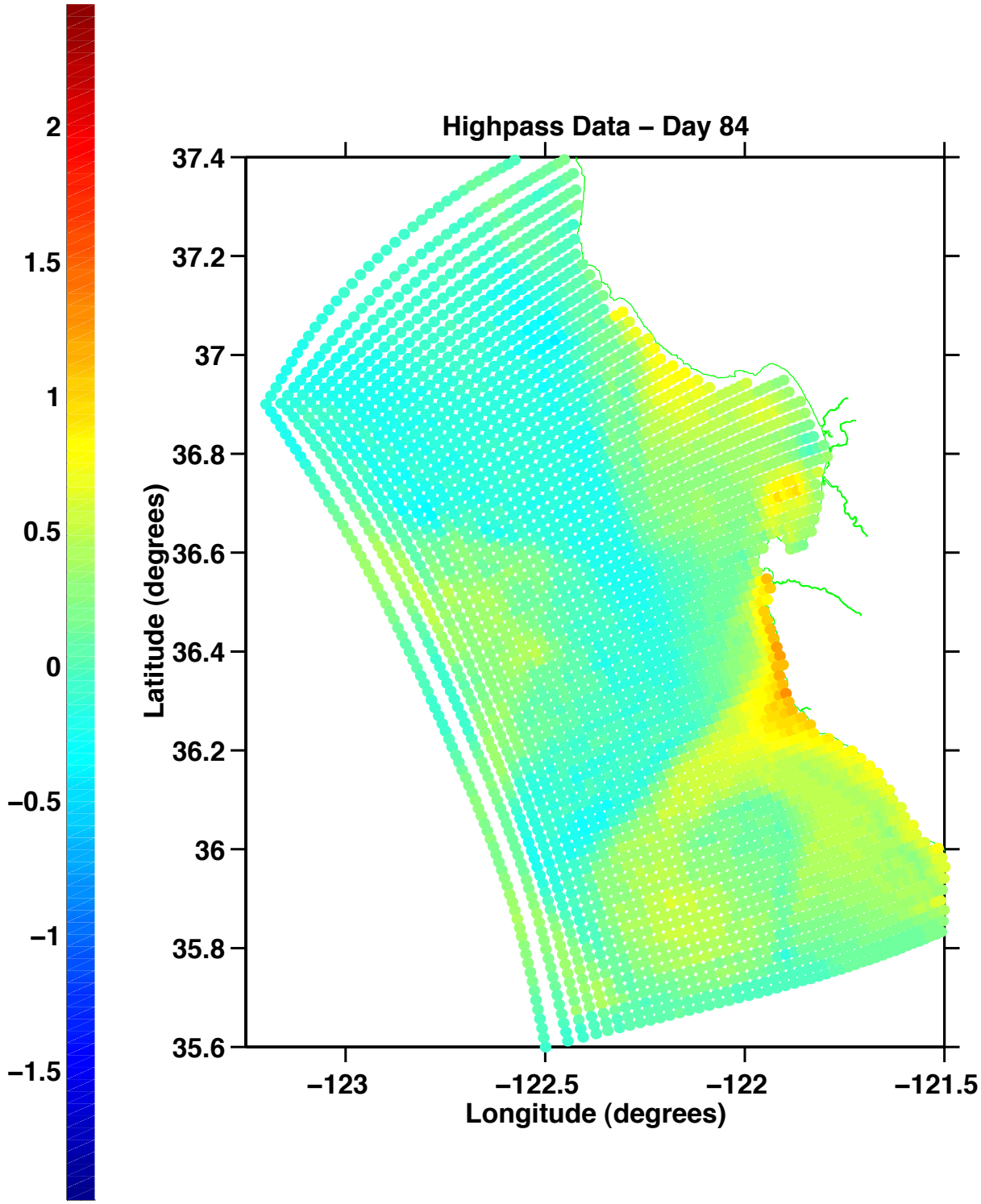

Figure 33. High pass filtered COAMPS-forced ICON model run from day 84 (25 March) 1999 showing concentration of warm water at Pt. Sur.

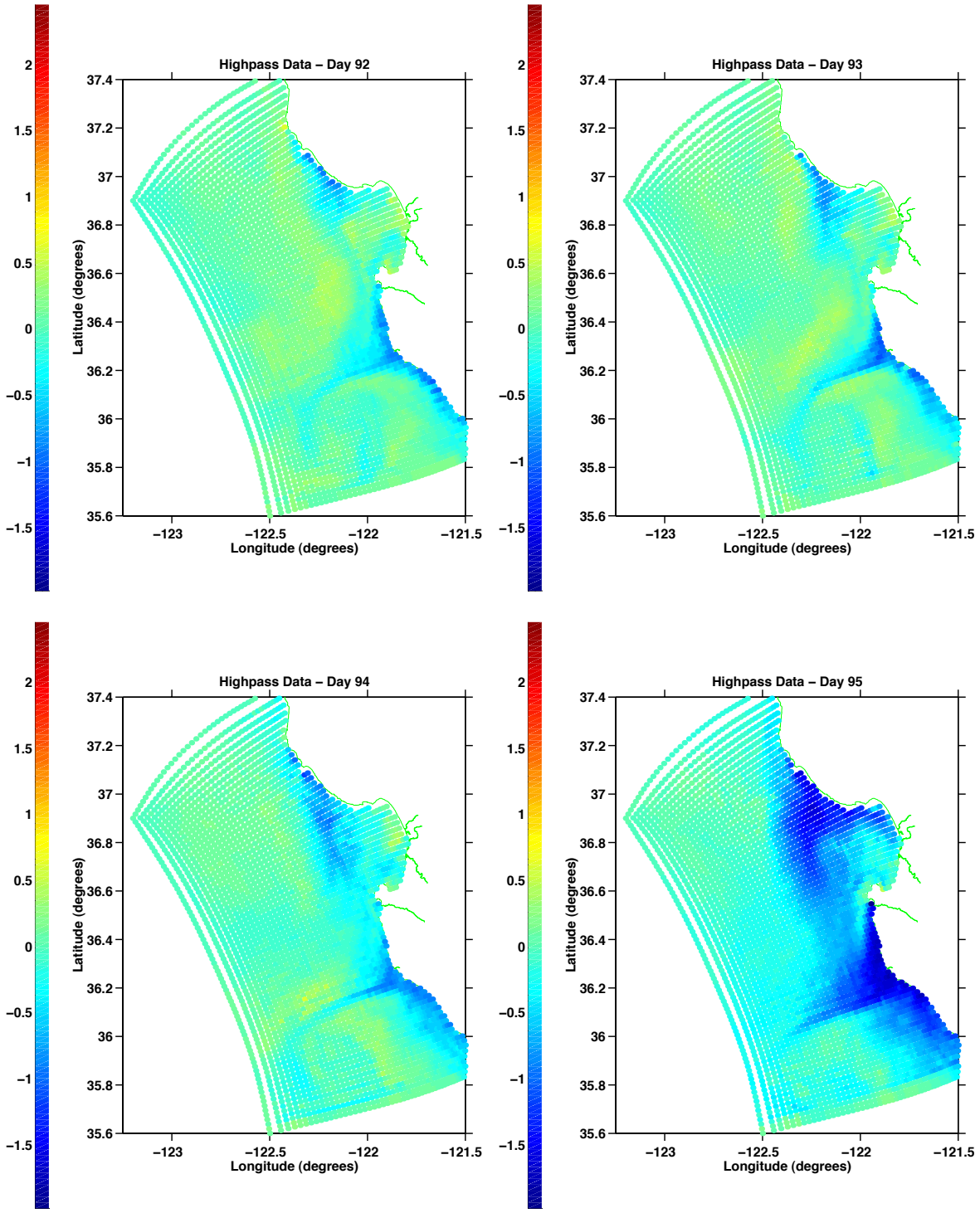

Figure 34. High pass filtered COAMPS-forced ICON model run for days 92-95 (3 April – 6 April) 1999 showing the progression of upwelled water.

IV. CONCLUSIONS

The original purpose of this project was to compare the forcing of the ICON ocean circulation model with 100 km NOGAPS wind fields and 9 km high resolution COAMPS wind fields. The occurrence of upwelling was analyzed along with how well individual upwelling events were resolved. Upwelling was the dominant feature studied, but several other mesoscale features were noticed in the ocean circulation model. These mesoscale features were: the presence of cold-water filaments extending from the coast into the open ocean, the formation and propagation of eddies throughout the model domain, and the presence of oceanic fronts. Overall, the 9 km resolution winds used in the COAMPS run produced many more of these features than the 100 km resolution winds used in the NOGAPS run. The 100 km NOGAPS wind fields did show stronger upwelling events, although they were much less intense and displayed a much weaker signature than the corresponding model run using the COAMPS wind fields. The features in either of the ICON model runs were not compared to actual oceanic conditions.

In the beginning of the paper some of the challenges involved with creating a coastal ocean circulation model were discussed. The most significant of these challenges were the complex and irregular coastline and topography, especially the interaction of the wind with coastal headlands. There have been several other studies on the interaction of winds with coastal headlands. The observations from these studies directly relate to the interactions noted in this thesis. Dorman et al. (1999) observed that "wind stress calculated directly from low aircraft legs is highest in the lee of large capes with peak values exceeding 0.7 N m^{-2}." They also note that the stress maxima along the California coast was spatially consistent with the region of coldest sea surface temperature observed by satellite (Dorman et al., 1999). This was consistent with what was observed in the ICON model runs, particularly around the Pt. Sur headland. The 9 km high resolution COAMPS wind fields displayed more of the effects of the coastline and topography than the 100 km NOGAPS wind fields. Also, the higher resolution winds produced more intense and localized upwelling features, sometimes displaying multiple local maximums depending on the variability of the coastal topography and coastline structure.

Specifically noticed were the effects characterized by the interaction between the high-resolution wind fields and the Pt. Sur headland. The high resolution winds created not only strong upwelling signatures, but also the interaction of those winds with the headland was the originating point for the cold water filaments that transported upwelled water away from the coast. The interaction between the winds and the headland created small eddies that would propagate north and south along the coast before moving westward and out of the model domain. The 9 km resolution wind fields displayed more detail and produced stronger headland effects.

There were some difficulties involved with the higher resolution wind fields. The 9 km COAMPS wind fields created more fluctuation within each upwelling event which caused some confusion in determining the end of one event and the beginning of another. For example, was a brief relaxation of the upwelling signature the end of a specific upwelling event, or was it a brief weakening of the winds within an event? Another element of difficulty was discovered when matching the surface velocity vector fields with the information displayed by the sea surface temperature fields. For example, during one or two of the upwelling time frames the temperatures were showing cold water along the coast and then transported within a filament to the west. When looking at the surface velocity vector daily plots, the movement of water was opposite, toward the coast suggesting downwelling. Because of friction and conservation of energy, the surface layer of water will lag behind what might be expected from upwelling or downwelling favorable winds. This transition time between upwelling and downwelling regimes could explain for the difference between the temperature fields and the surface velocity vectors.

The COAMPS wind fields were not available for the case study time frame, but were available beginning in May of 1999. In an attempt to show a correlation between the COAMPS-predicted winds and the COAMPS-forced ICON model, the COAMPS winds and calculated wind stress curl were plotted for year day 132 (12 May) (Figure 35). This is outside of the time frame of the case study discussed previously, but it gives a good indication of how the winds match up to what is being predicted by the ICON model run. The COAMPS winds show critical influence from the complex coastline and topography structure. The bending of the winds into Monterey Bay (sea breeze) equated

to a positive wind stress curl in the northern upwelling location. The interaction between the positive wind stress curl and the ocean surface creates upwelling through divergence of Ekman transport (deflection from the winds 90° to the right in the Northern Hemisphere). The positive wind stress curl was also noticed in the southern upwelling location as the winds bent around the Pt. Sur headland and displayed a much higher intensity than in the northern upwelling location. The sea surface temperature from the COAMPS-forced ICON model run (Figure 36) showed a very broad region of cold water due to extensive upwelling in both the northern and southern upwelling locations Also shown is the surface velocity vectors from the COAMPS-forced ICON model run (Figure 37) which showed the ocean surface movement during that day. There was very strong along coast surface current movement in the southern direction which was consistent with an upwelling event. The 100 km NOGAPS wind fields had a much lower resolution and the ICON model only had one or two NOGAPS grid points within the model domain. This would not allow for the calculation of wind stress curl. Because the 9km COAMPS wind fields had a much higher resolution there was sufficient resolution to see a coastal headland effect.

A field program was carried out in Monterey Bay in August 2000 by ICON partners in which observations were collected that support the results of this study. During the MBARI Upper-Water Column Science Experiment (MUSE), a research aircraft was used to map winds and air temperature at 130 meters above Monterey Bay, along with sea surface temperature from a downward-looking radiometer. Finding a direct correlation between wind stress and wind stress curl, and its effects on ocean circulation and upwelling events, could prove very useful in modeling efforts. An example of the observed wind stress is seen in Figure 38, which displays a low level wind jet near the Pt. Santa Cruz upwelling location discussed throughout the paper. Warm air moving from over land to over the ocean is pushing the cold water away from the coast and to the south. On the figure the aircraft-derived winds at 130 meter altitude are displayed to outline the wind jet, and the CODAR surface currents are shown to illustrate the surface circulation. Zemba and Friehe (1987) attributed the vertical structure of similar wind jets to a combination of drag with the sea surface and thermal wind due to horizontal temperature gradients. This would explain the spatial variation between the

area of high winds and the corresponding region of cold ocean water influenced by the wind. The wind stress curl was computed (Figure 39) and the maximum values (outlined in blue) can be seen in the area of the strongest gradient and largest wind shift. Another illustration of the wind shift can be seen in the red vectors extending from the M3, M2 and M1 buoy locations. This illustrates the decrease in winds and the wind shift as you move toward shore from the buoy farthest from shore to the buoy located within Monterey Bay. The presence of the Santa Cruz Mountains causes a sheltering effect for the northern portion of the Monterey Bay and shadows the winds within the bay.

Within the course of the comparison between the NOGAPS and the COAMPS wind forcing the question arises; what is it about the difference in wind fields that are producing even more intense and localized upwelling features and are these features mirroring what is shown through observations? Future work related to this topic could include identifying mechanisms that cause differences in the modeled ocean circulation. In particular, the correlation between wind stress curl in each of the upwelling locations to the strength of the upwelling event. Other investigations could include any coastal orographic effects and the discovery of any other mechanisms identified through further study. A final element included in a future study could be comparing the results of the model runs to observed conditions. This would prove helpful in determining whether the COAMPS 9 km wind fields are more accurate.

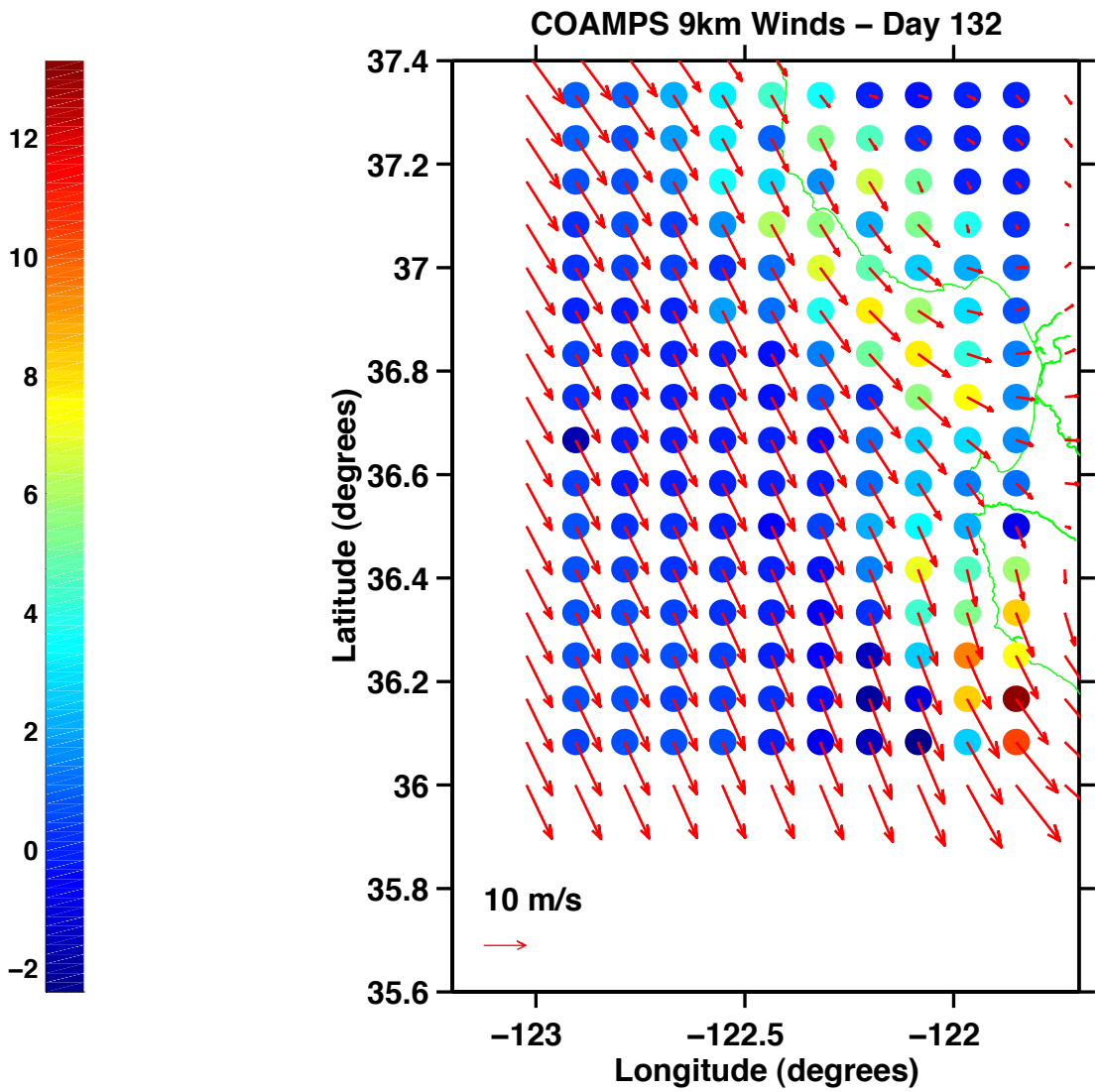

Figure 35. 9 km COAMPS winds and computed wind stress curl from COAMPS run for day 132 (12 May) 1999.

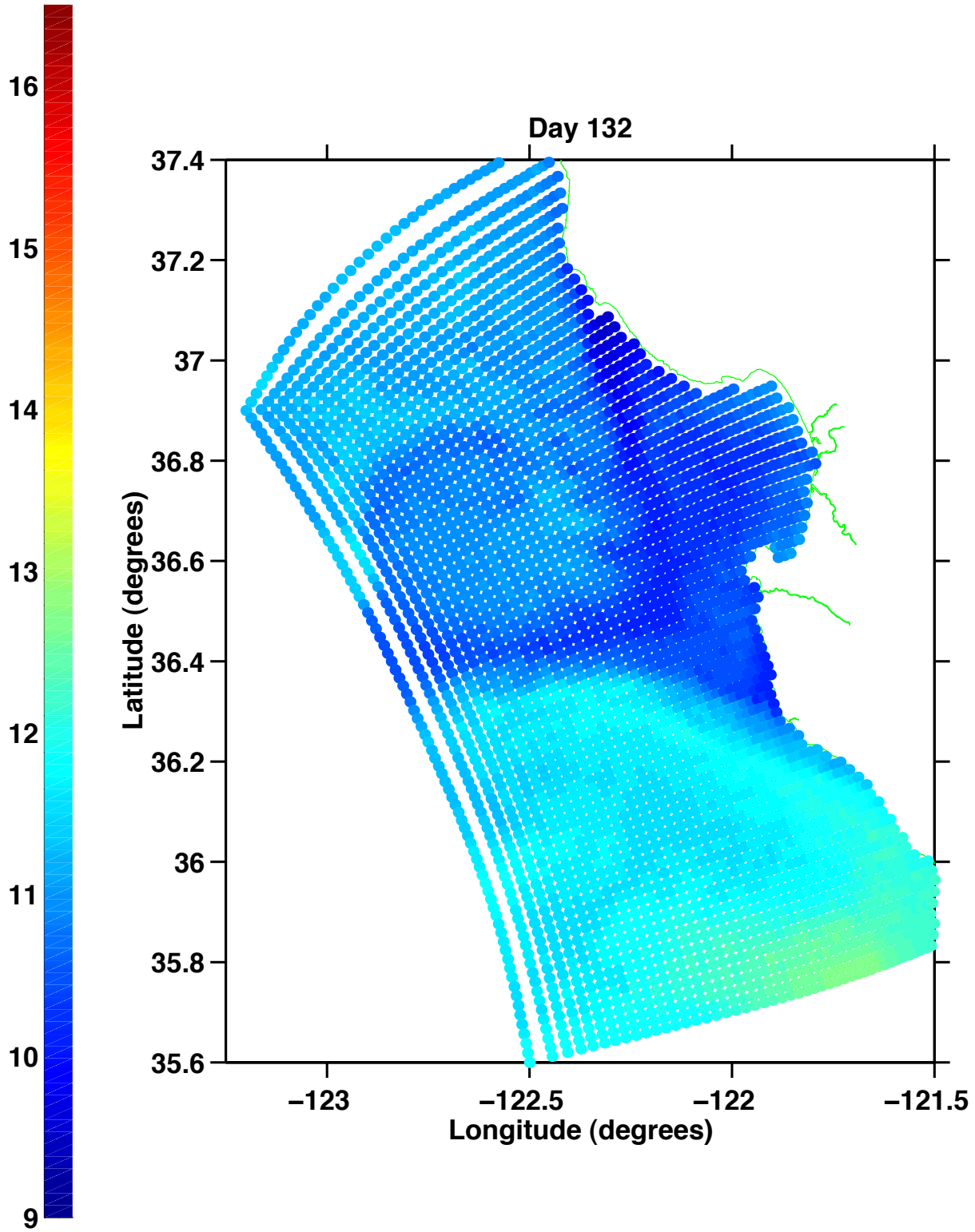

Figure 36. SST for COAMPS-forced ICON model run from day 132 (12 May) 1999 showing upwelled cold water at Pt. Sur.

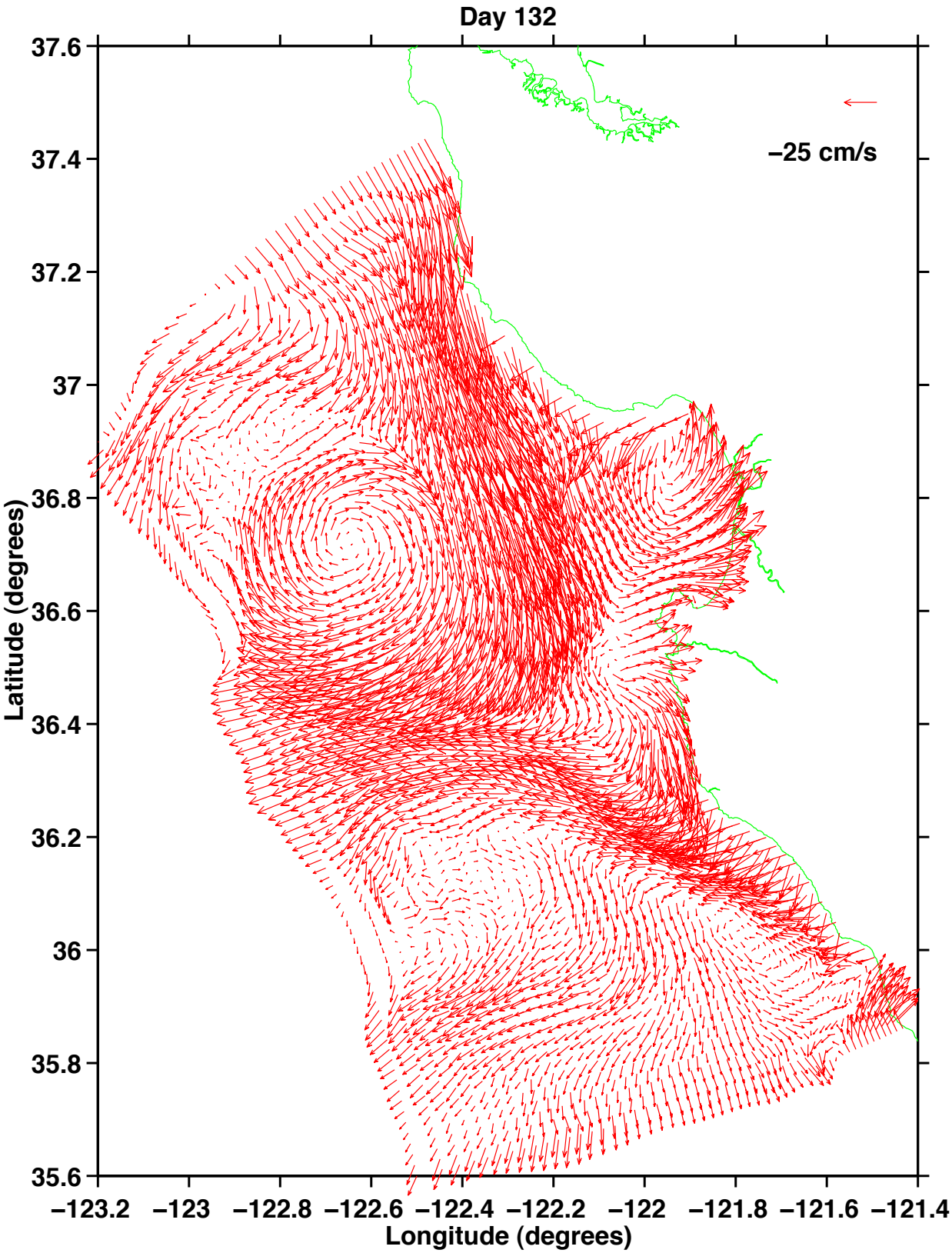

Figure 37. Surface velocity vectors for COAMPS-forced ICON model run from day 132 (12 May) 1999 showing upwelled cold water at Pt. Sur.

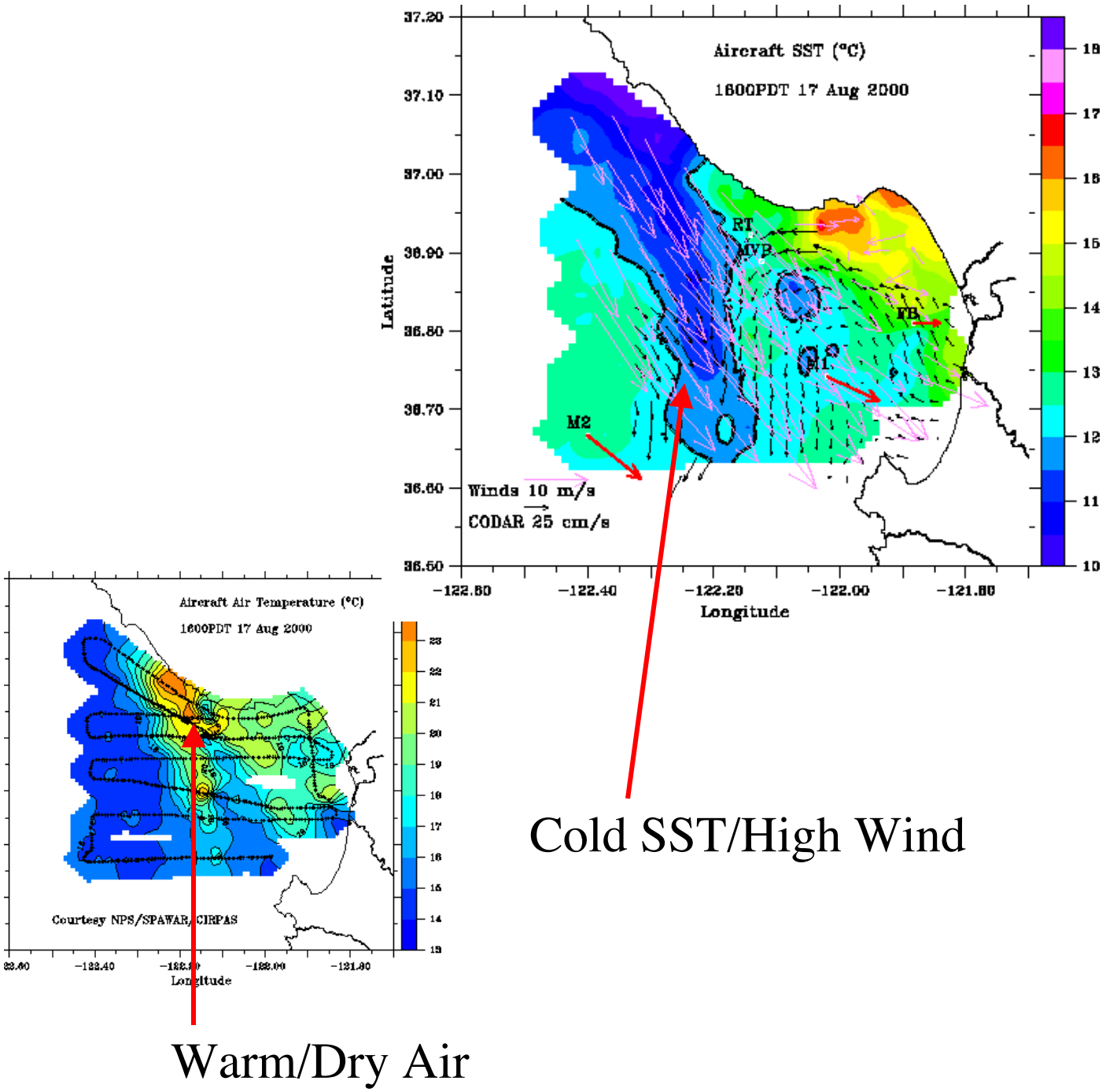

Figure 38. Aircraft derived winds, SST, and air temperature near Pt. Santa Cruz.

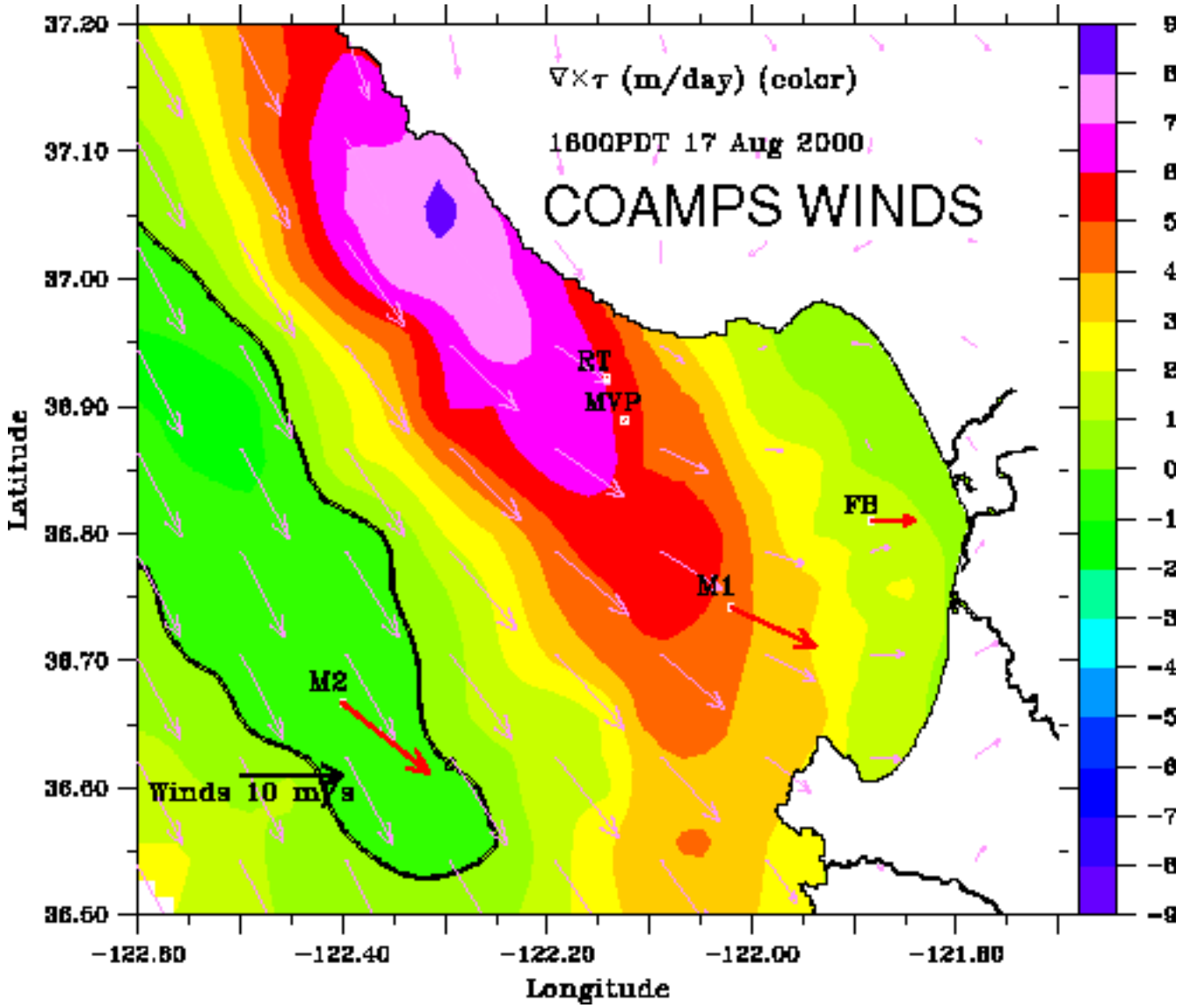

Figure 39. Wind stress curl near Pt. Santa Cruz.

THIS PAGE INTENTIONALLY LEFT BLANK

LIST OF REFERENCES

1. Arakawa, A., and V. R. Lamb, 1977. Computational Design of the Basic Dynamical Processes of the UCLA General Circulation Model. Methods in Computational Physics, 17, Academic Press, Inc. New York, 173-265.

2. Baker, N., E. Barker, R. Daley, R. Gelaro, J. Goerss, T. Hogan, R. Langland, R. Pauley, M.A. Rennick, C. Reynolds, G. Rohaly, T. Rosmond, S. Swadley, 1998. The Navy Operational Global Atmospheric Prediction System: A Brief History of Past, Present, and Future Developments – 1998. NRL website (www.nrlmry.navy.mil/cgi-bin/print_hit_bold.pl/aboutnrl/nogaps_history.html).

3. Blumberg, A. F., G. L. Mellor, 1987. A description of a Three-Dimensional Coastal Ocean Circulation Model. In Heaps, N.S. (Ed.), Coastal and Estuarine Sciences 4: Three Dimensional Coastal Models. AGU, Washington, D.C., 1-16.

4. Clancy, R. M., P. W. deWitt, P. May, D. -S. Ko, 1996. Implementation of a Coastal Ocean Circulation Model for the West Coast of the United States. Proceedings of the American Meteorological Society Conference on Coastal Oceanic and Atmospheric Prediciton, Atlanta, GA., 72-75.

5. Clancy, R. M. and P. J. Martin, 1981. Synoptic Forecasting of the Oceanic Mixed Layer Using the Navy's Operational Environmental Data Base. Present Capabilities and Future Applications. Bulletin of the American Meteorological Society, 67, 770-784.

6. Clancy, R. M. and K. D. Pollak, 1983. A Real-Time Synoptic Ocean Thermal Analysis Forecast System. Progressive Oceanography, 12, 383-424.

7. Clancy, R. M. ,J. E. Kaitala, L. F. Zambresky, 1986. The Fleet Numerical Oceanographic Center Global Spectral Ocean Wave Model. Bulletin of the American Meteorological Society, 67, 498-512.

8. Collins, C. A., N. Garfield, T. A. Rago, F. W. Rishmiller, E. Carter, 2000. Mean Structure of the Inshore Countercurrent and California Undercurrent of Point Sur, California. Deep-Sea Research II, 765-782.

9. Dorman, C. E., T. Holt, D. P. Rogers, K. Edwards, 1999; Large Scale Structure of the June-July 1996 Marine Boundary Layer Along California and Oregon. Monthly Weather Review, 128, 1632-1652.

10. Gerson, D. J., 1975. A numerical Ice Forecasting System. Tech. Rep. NOO RP 8, 138 pp. [Available from The Naval Oceanographic Office, NSTL Station, MS 39529.

11. Harrison, E. J., 1981. Initial Results from the Navy Two-Way Interactive Nested Tropical Cyclone Model. Monthly Weather Review, 109, 173-177.

12. Heburn, G. W., and R. C. Rhodes, 1987. Numerical Simulations of Wind Forced Seasonal and Interannual Variability of the Transport Through the Caribbean Sea. Trans. Amer. Geophys. Union, 68, 337 pp.

13. Hibler, W. D., 1979. A Dynamic Thermodynamic Sea Ice Model. Journal of Physical Oceanography, 9, 815-846.

14. Hodur, R. M., 1996. The Naval Research Laboratory's Coupled Ocean/Atmosphere Mesoscale Prediction System (COAMPS). Monthly Weather Review, 125, 1414-1430.

15. Hodur, R. M., 1987. Evaluation of a Regional Model with an Update Cycle. Monthly Weather Review, 115, 2707-2718.

16. Hodur, R. M. and S. D. Burk, 1978. The Fleet Numerical Weather Central Tropical Cyclone Model: Comparison of Cyclic and One-Way Interactive Boundary Conditions. Monthly Weather Review, 106, 1665-1671.

17. Hogan, T. F., and T. E. Rosmond; The Description of the Navy Operational Global Atmospheric Prediction System's Spectral Forecast Model. Monthly Weather Review, 119, 1786-1815.

18. Ko, D. -S., R. A. Allard, E. J. Metzger, R. C. Rhodes, 1996. A Coupled West Coast Model With Seasonal Forcing. Eos, (suppl.), 76, 3, OS38.

19. Lewis, J. K., I. Shulman, A. F. Blumberg, 1998. Assimilation of CODAR Observations into Ocean Models. Continental Shelf Research, 18, 541-559.

20. Ly, L. N., P. Luong, J. D. Paduan, D. Karacin, 1999. Response of the Monterey Bay Region to Wind Forcing by An Atmospheric Model. Proceedings of the 3RD Conference on Coastal Atmospheric and Oceanic Prediction and Processes, New Orleans, LA., 76-79.

21. Lynn, R. J., J. J. Simpson, 1987. The California Current System: The Seasonal Variability of its Physical Characteristics. Journal of Geophysical Research, 92, 12947-12966.

22. Paduan, J. D. and L. K. Rosenfeld, 1996. Remotely Sensed Surface Currents in Monterey Bay from Shore-Based HF radar (Coastal Ocean Dynamics Application Radar). Journal of Geophysical Research, 101, 20669-20686.

23. Petruncio, E. T., L. K. Rosenfeld, J. D. Paduan, 1998. Observations of the Internal Tide in Monterey Canyon. Journal of Physical Oceanography, 28, 1873-1903.

24. Righi, D. D., P. T. Strub, J. C. Kindle, 1999. Validation of a California Current Model Through Comparison with Altimeter and Drifter Circulation Statistics. Proceedings of the 3RD Conference on Coastal Atmospheric and Oceanic Prediction and Processes, New Orleans, LA, 1999, 97-100.

25. Rosenfeld, L. K., F. B. Schwing, N. Garfield, D. E. Tracy, 1994. Bifurcated Flow from an Upwelling Center: A Cold Water Source for Monterey Bay. Continental Shelf Research, 14, 931-964.

26. Rosenfeld, L. K., J. D. Paduan, E. T. Petruncio, J. E. Concalves, 1999. Numerical Simulations and Observations of the Internal Tide in a Submarine Canyon. Proceedings 'Aha Huliko'a Hawaiian Winter Workshop', University of Hawaii at Manoa, 1-8.

27. Shulman, I., C. –R. Wu, J. K. Lewis, J. D. Paduan, L. K. Rosenfeld, S. R. Ramp, M. S. Cook, J. C. Kindle, D. -S. Ko, 1999. Development of the High Resolution, Data Assimilating Numerical Model of the Monterey Bay. Estuarine and Coastal Modeling, 980-994.

28. Shulman, I, C. –R. Wu, J. K. Lewis, J. D. Paduan, L. K. Rosenfeld, J. D. Kindle, S. R. Ramp, C. A. Collins, 2001. High Resolution Modeling and Data Assimilation in the Monterey Bay Area. Continental Shelf Research, In Press.

29. What is COAMPS?; NRL website (www.nrlmry.navy.mil/projects/coamps/data/overview/index.html).

30. Zemba J., and C. A. Friehi, 1987. The Marine Atmospheric Boundary Layer Jet in the Coastal Ocean Dynamics Experiment. Journal of Geophysical Research, 92, 1489-1496.

THIS PAGE INTENTIONALLY LEFT BLANK

INITIAL DISTRIBUTION LIST

1. Defense Technical Information Center
   8725 John J. Kingman Road, Suite 0944
   Ft. Belvoir, VA 22060-6218

2. Dudley Knox Library
   Naval Postgraduate School
   411 Dyer Road
   Monterey, CA 93943-5101

3. Dr. Igor Shulman
   Institute of Marine Sciences
   University of Southern Mississippi
   Stennis Space Center, MS 39529
   Shulman@coam.usm.edu

4. Dr. John C. Kindle
   Oceanography Division
   Naval Research Laboratory
   Stennis Space Center, MS 39529
   kindle@nrlssc.navy.mil

5. LT David G. Blencoe
   dgblenco@nps.navy.mil